NATIONAL ADVISORY COMMITTEE
FOR AERONAUTICS

TECHNICAL NOTE 2743

LANDING-GEAR IMPACT

By W. Flügge

Stanford University

NACA

Washington

October 1952

1C

NATIONAL ADVISORY COMMITTEE FOR AERONAUTICS

TECHNICAL NOTE 2743

LANDING-GEAR IMPACT

By W. Flügge

SUMMARY

This report deals with the impact forces in landing gears. Both the landing impact and the taxying impact have been considered, but drag forces have been so far excluded. The differential equations are developed and their numerical integration is shown, considering the nonlinear properties of the oleo shock strut. A way is shown how the dimensions of the metering pin may be determined from a given load-time diagram. A review of German literature on landing-gear impact is also presented.

INTRODUCTION

The objective of this report is to study the impact forces acting on the wheels and shock struts of an airplane. For practical reasons the investigation has been limited to the vertical forces and does not consider the effect of the drag load which acts on the wheels during the spin-up time. Within the limits drawn by this restriction, an attempt has been made to develop a method for numerical computations which, it is hoped, will be useful in practical design work.

The oleo-pneumatic shock strut which is now in general use and which has attained a high degree of perfection exhibits a rather complicated relation between the force, the stroke, and the rate of stroke. For practical work, it is imperative to express this relation in mathematical form and to develop a method for the numerical solution of the ensuing differential equations. A detailed discussion of this subject will be found in the section "Intentional Nonlinearities."

Nevertheless it is sometimes useful to consider a highly idealized type of landing gear which has linear differential equations. Although such a model will never correctly reproduce the details of the real landing impact, it admits of easy mathematical treatment and permits study of questions of a more general character. This has been done in the section "Linear Spring-Damper Systems" and the usefulness of the results obtained there lies in the fact that they do not depend on the more or less incidental details of real landing gears which unavoidably enter the computations of the nonlinear theory.

The later sections of the report are devoted to refinements of the method. Except for the simple mass corrections, they will not be used in daily routine work, but they may be of particular importance when airplanes of unusual design are built.

SYMBOLS

A_n, B_n	coefficients
A_0	inner cross section of barrel at oil level
A_1	total cross section of piston
A_2	inner cross section of piston
A_3	area of gap between metering pin and edge of orifice
a, b	distances of landing gears from center of gravity (used only in section "The Airplane as a Whole")
b	damping constant for one shock strut (used only in section "Linear Spring-Damper Systems")
F_0	force in strut when strut is fully expanded and at rest
F_1	compressive force in shock strut
F_2	compressive force between wheel and ground (if different from F_1)
F_3	force in auxiliary landing gear
g	acceleration due to gravity

h   height of obstacle encountered during taxying

I_x, I_y moment of inertia of airplane with respect to longitudinal and lateral axis, respectively

$$i_x = \sqrt{I_x/m}$$
$$i_y = \sqrt{I_y/m}$$
radii of gyration

k_1 spring constant for one shock strut

k_2 spring constant for one tire

m   mass of airplane

m_1 that part of mass m attributed to one landing gear

m_2 unsprung mass for one landing gear .

p_0 pressure in both chambers when strut is fully expanded and at rest

p_1 pressure in upper chamber of strut

p_2 pressure in lower chamber of strut

T   reference time

t   time

V   vertical velocity of landing gear when it first touches ground

v   oil velocity in orifice

W   vertical force, other than impact force, acting on airplane (weight minus lift)

W_1 that part of force W attributed to one landing gear

x   stroke of shock strut

x_1 vertical displacement of mass m_1

x_2 vertical displacement of unsprung mass m_2

x_3 used instead of x_1 when a second landing gear must be
considered simultaneously

z displacement of center of gravity of airplane

α angular displacement (angle of pitch) of airplane in its
plane of symmetry

γ ratio of specific heats

δ static deflection of mass m_1

ρ density of oil

All displacements are zero when the wheels touch the ground without
pressure.

LINEAR SPRING-DAMPER SYSTEMS

Differential Equations

Essentially, a landing gear consists of a shock strut and a wheel
with a tire. The shock strut may be compressed considerably. It opposes
this deformation with an elastic force increasing with increasing stroke
and with a damping force which depends on the rate of stroke and which
dissipates mechanical energy. This shock strut may be represented by a
spring and a damper arranged in parallel (fig. 1). The tire is for the
present purposes a simple spring whose deformation is more or less pro-
portional to the applied force.

Between these two deformable elements there is the mass m_2 of
the wheel, including those parts of the shock strut which participate in
the motion of the wheel. On top of the whole landing gear there is the
airplane mass or, more exactly, that portion m_1 of the airplane mass
which belongs to the landing gear under consideration.

When the airplane lands, this system approaches the ground with a
considerable velocity. As long as the spinning up of the wheels is not
considered, only the vertical component V of this velocity is of
interest. The impact begins when the lower end of the landing gear
touches the ground. This instant is designated $t = 0$, and the vibra-
tions of the masses m_1 and m_2 are studied which follow for $t > 0$
when the motion of the lower end of the spring-mass system is suddenly
stopped.

Linear differential equations are obtained when the shock strut is replaced by a simple spring and a viscous damper (dashpot) and when the tire is assumed to be a linear spring. There might also be a linear damper coupled with the tire but, compared with the shock-strut damping, the contribution of the tire to damping is so small that it does not seem worth while to include it in the equations.

The differential equations of the landing-gear impact will now be formulated. Figure 2 shows the mechanical system in two positions, one for $t = 0$ and the other for some later time. The displacements of the masses m_1 and m_2, measured from their positions at $t = 0$, are called x_1 and x_2, respectively. Their difference

$$x = x_1 - x_2$$

is the stroke of the shock strut.

If k_2 is the spring constant of the tire, then the force transmitted from the ground to the unsprung mass m_2 is

$$F_2 = k_2 x_2 \tag{1a}$$

On the other hand, the force in the shock strut is the sum of an elastic force $k_1 x$ and of a damping force which, in linear theory, must be assumed proportional to the velocity $\dot{x} = dx/dt$ with which the masses m_1 and m_2 approach each other:

$$F_1 = k_1 x + b\dot{x} \tag{1b}$$

The third force is the load W_1 which acts as an external force on the mass m_1. It is a part of the weight of the airplane minus a corresponding part of the wing lift. It will be shown in the section "The Airplane as a Whole" what part of the total weight and lift must be attributed to each landing gear.

The three forces W_1, F_1, and F_2 determine the motion of the masses m_1 and m_2, according to the equations

$$m_1 \ddot{x}_1 = W_1 - F_1$$

$$m_2 \ddot{x}_2 = F_1 - F_2$$

When F_1 and F_2 are expressed here by x and x_2 according to equations (1a) and (1b), or better still by x_1 and x_2, the differential equations of the linear landing gear are obtained:

$$m_1\ddot{x}_1 + b\left(\dot{x}_1 - \dot{x}_2\right) + k_1\left(x_1 - x_2\right) = W_1 \tag{2a}$$

$$m_2\ddot{x}_2 - b\left(\dot{x}_1 - \dot{x}_2\right) - k_1\left(x_1 - x_2\right) + k_2 x_2 = 0 \tag{2b}$$

The problem is of the fourth order and requires four initial conditions for $t = 0$. Before its solution is given, a simplified version will be considered which is sufficient in most cases.

Solution Neglecting Unsprung Mass

The unsprung mass m_2 is rather small, usually between 2 and 5 percent of the mass m_1. Under certain conditions it has a very definite influence on the force in the landing gear. But it will be seen that it is only of minor importance for the early phase of the landing impact, up to and beyond the maximum of the impact force. One may therefore begin with a simplified set of differential equations, obtained from equations (2) by dropping the term with m_2:

$$m_1\ddot{x}_1 + b\left(\dot{x}_1 - \dot{x}_2\right) + k_1\left(x_1 - x_2\right) = W_1 \tag{3a}$$

$$-b\left(\dot{x}_1 - \dot{x}_2\right) - k_1\left(x_1 - x_2\right) + k_2 x_2 = 0 \tag{3b}$$

Since $\ddot{x}_1$ and $\dot{x}_2$ are the highest derivatives occurring in these equations, the problem is of the third order, and there must be three initial conditions.

Two of them follow from the fact that the displacements x_1 and x_2 are counted from the position of the system at $t = 0$. Therefore

$$t = 0: \qquad x_1 = 0, \qquad x_2 = 0$$

The third condition is that the mass m_1 has at this time the velocity V:

$$t = 0: \qquad \dot{x}_1 = V$$

It is useful to replace the second condition by an equation for x_1. This may easily be done by introducing all three conditions in the differential equations. Equation (3b) yields $\dot{x}_2 = V$, and it is seen here that this is not an independent fourth condition, as one might feel inclined to think. Equation (3a) yields now:

$$t = 0: \qquad \ddot{x}_1 = W_1/m_1$$

and this initial relation may be used instead of any one of the other three, preferably instead of $x_2 = 0$.

One may easily find a particular solution of differential equations (3):

$$\left. \begin{aligned} x_1 &= W_1 \frac{k_1 + k_2}{k_1 k_2} \\[2em] x_2 &= \frac{W_1}{k_2} \end{aligned} \right\} \tag{4}$$

It describes the position in which the system is in equilibrium under the load W_1. Besides this, the solution of the homogeneous equations is needed. Since all coefficients of the equations are constant, the homogeneous solutions are exponential functions of time, say

$$x_1 = Ae^{\lambda t}$$

$$x_2 = Be^{\lambda t}$$

When this solution is introduced into equations (3a) and (3b) after dropping there the term W_1, two linear equations are found for A and B:

$$A\left(m_1\lambda^2 + b\lambda + k_1\right) - B\left(b\lambda + k_1\right) = 0$$

$$A\left(b\lambda + k_1\right) - B\left(b\lambda + k_1 + k_2\right) = 0 \qquad\qquad (5)$$

Since these equations are homogeneous, they will not have a solution $A \neq 0$, $B \neq 0$ unless the determinant of the coefficients vanishes, and this condition yields the characteristic equation of the problem:

$$\lambda^3 + \frac{k_1 + k_2}{b}\lambda^2 + \frac{k_2}{m_1}\lambda + \frac{k_1 k_2}{m_1 b} = 0 \qquad\qquad (6)$$

It is of the third degree. One of its three roots must be real and, since all coefficients are positive, this root must necessarily be negative, say

$$\lambda = -\lambda_3$$

The other two roots may also be real and negative,

$$\lambda = -\lambda_1$$

and

$$\lambda = -\lambda_2$$

or they may be conjugate complex:

$$\lambda = -\mu \pm i\nu$$

It may easily be shown that in this case the real part must be negative, $-\mu$.

For the rest of the formal treatment the cases of real and of complex roots λ must be separated.

High damping, all roots real.- In the case of high damping with all roots real the general solution of differential equations (3) is

$$
\left.
\begin{aligned}
x_1 &= W_1\,\frac{k_1 + k_2}{k_1 k_2} + A_1 e^{-\lambda_1 t} + A_2 e^{-\lambda_2 t} + A_3 e^{-\lambda_3 t}\\[2em]
x_2 &= W_1\,\frac{1}{k_2} + B_1 e^{-\lambda_1 t} + B_2 e^{-\lambda_2 t} + B_3 e^{-\lambda_3 t}
\end{aligned}
\right\} \tag{7}
$$

In these formulas only the constants A_1, A_2, and A_3 may be chosen arbitrarily, while B_1, B_2, and B_3 depend on them through equations (5), in which in each case the appropriate λ must be inserted.

When t is set equal to zero and then x_1 and its derivatives are introduced in the initial conditions, a set of three linear equations is obtained for A_1, A_2, and A_3. They are:

$$
A_1 + A_2 + A_3 = -W_1\left(\frac{1}{k_1} + \frac{1}{k_2}\right)
$$

$$
\lambda_1 A_1 + \lambda_2 A_2 + \lambda_3 A_3 = -V
$$

$$
\lambda_1^2 A_1 + \lambda_2^2 A_2 + \lambda_3^2 A_3 = \frac{W_1}{m_1}
$$

They must be solved numerically, and then the displacements may be found for any time t.

The most interesting quantities are the stroke $x = x_1 - x_2$ and the impact force F_1. For both the B's are needed in terms of the A's:

$$
B_n = A_n\,\frac{k_1 - b\lambda_n}{k_1 + k_2 - b\lambda_n} \qquad n = 1,\,2,\,3 \tag{8}
$$

and then

$$
x = \frac{W_1}{k_1} + \frac{A_1 k_2}{k_1 + k_2 - b\lambda_1}\,e^{-\lambda_1 t} + \frac{A_2 k_2}{k_1 + k_2 - b\lambda_2}\,e^{-\lambda_2 t} + \frac{A_3 k_2}{k_1 + k_2 - b\lambda_3}\,e^{-\lambda_3 t}
$$

and

$$F_1 = F_2$$

$$= k_2 x_2$$

$$= W_1 + k_2 \left(B_1 e^{-\lambda_1 t} + B_2 e^{-\lambda_2 t} + B_3 e^{-\lambda_3 t} \right)$$

The coefficients B_n need not necessarily be positive. Then there may occur a time $t > 0$, where $F_2 = 0$. If this happens, it would terminate the domain of validity of the formulas. For greater values of t, the force F_2 would not become negative (i.e., tensile), but the wheel would leave the ground; the airplane would rebound.

Because of the force W_1, the airplane would soon return to the ground. Meanwhile its horizontal speed or the angle of attack might have decreased and hence W_1 increased. The vertical velocity at the second impact would be, on the other hand, considerably smaller than V. The new impact would therefore be less violent, but not necessarily uninteresting, because it would find the shock strut in a less favorable condition, with $x > 0$ and, perhaps, close to the possible limit.

Whether rebounding will occur and how strong the second impact will be can be determined only from detailed numerical computations in each particular case. But one may say quite generally that the probability of a zero of F_2 is greater the more solutions the homogeneous equations have. Since each additional mass and each additional spring increases the order of the equations, one should avoid mechanical complexity if rebounding is undesirable.

Low damping, one pair of roots complex.- The complex exponentials which appear in the case of low damping with one pair of roots complex may be expressed in real form by exponential and trigonometric functions:

$$\left. \begin{aligned} x_1 &= W_1 \frac{k_1 + k_2}{k_1 k_2} + e^{-\mu t} \left(A_1 \cos \nu t + A_2 \sin \nu t \right) + A_3 e^{-\lambda_3 t} \\[2em] x_2 &= W_1 \frac{1}{k_2} + e^{-\mu t} \left(B_1 \cos \nu t + B_2 \sin \nu t \right) + B_3 e^{-\lambda_3 t} \end{aligned} \right\} \quad (9)$$

The relations between the A's and the B's are here more involved because equation (8) can be applied only before the trigonometric functions are introduced. When this is done the following relations are found:

$$B_1 = \left(1 + \alpha_1\right)A_1 + \beta_1 A_2$$

$$B_2 = -\beta_1 A_1 + \left(1 + \alpha_1\right)A_2$$

$$B_3 = \left(1 + \alpha_2\right)A_3$$

with

$$\alpha_1 = m_1 \frac{\mu^2\left(k_1 - b\mu\right) - \nu^2\left(k_1 + b\mu\right)}{\left(k_1 - b\mu\right)^2 + b^2\nu^2}$$

$$\beta_1 = m_1 \frac{b\nu\left(\mu^2 + \nu^2\right) - 2k_1\mu\nu}{\left(k_1 - b\mu\right)^2 + b^2\nu^2}$$

$$\alpha_2 = \frac{m_1\lambda_3^2}{k_1 - b\lambda_3}$$

The boundary conditions will now yield the following set of three equations for A_1, A_2, and A_3:

$$A_1 + A_3 = -W_1\left(\frac{1}{k_1} + \frac{1}{k_2}\right)$$

$$\mu A_1 - \nu A_2 + \lambda_3 A_3 = -V$$

$$\left(\mu^2 - \nu^2\right)A_1 - 2\mu\nu A_2 + \lambda_3^2 A_3 = \frac{W_1}{m_1}$$

When these equations have been solved numerically, B_1, B_2, and B_3 may be found from the preceding formulas. Then

$$x = x_1 - x_2$$

$$= \frac{W_1}{k_1} - \frac{A_3 m_1 \lambda_3^2}{k_1 - b\lambda_3} e^{-\lambda_3 t} - \left(\alpha_1 A_1 + \beta_1 A_2\right)e^{-\mu t} \cos \nu t +$$

$$\left(\beta_1 A_1 - \alpha_1 A_2\right)e^{-\mu t} \sin \nu t \qquad\qquad (10)$$

$$F_1 = F_2$$

$$= k_2 x_2$$

$$= W_1 + k_2\left[B_3 e^{-\lambda_3 t} + e^{-\mu t}\left(B_1 \cos \nu t + B_2 \sin \nu t\right)\right]$$

In this case rebounding is rather probable because of the trigonometric terms, and it will be inevitable when $W_1 = 0$.

Solution Not Neglecting Unsprung Mass

The results just described may be considered representative for the landing impact if it can be shown that they are not seriously affected by the neglected mass m_2 of the wheel. This side of the problem will now be investigated.

Instead of equations (3) set (2) must be used which still contains the term with m_2. Four initial conditions are required:

$$t = 0: \qquad x_1 = 0, \qquad x_2 = 0, \qquad \dot{x}_1 = V, \qquad \dot{x}_2 = V$$

which now are all independent of each other. When they are introduced
into differential equations (2), there are obtained

$$t = 0: \qquad \ddot{x}_1 = W_1/m_1, \qquad \ddot{x}_2 = 0$$

If equation (2a) is differentiated once more and again everything known
is introduced, another dependent condition is found:

$$t = 0: \qquad \dddot{x}_1 = -\frac{bW_1}{m_1^2}$$

For actual use, choose from all these conditions the set of four which
refer to x_1 only:

$$t = 0: \qquad x_1 = 0, \qquad \dot{x}_1 = V, \qquad \ddot{x}_1 = \frac{W_1}{m_1}, \qquad \dddot{x}_1 = -\frac{bW_1}{m_1^2} \qquad (11)$$

The general solution of equations (2) is

$$x_1 = W_1 \frac{k_1 + k_2}{k_1 k_2} + e^{-\mu_1 t}\left(A_1 \cos \nu_1 t + A_2 \sin \nu_1 t\right) +$$

$$e^{-\mu_2 t}\left(A_3 \cos \nu_2 t + A_4 \sin \nu_2 t\right) \qquad (12a)$$

$$x_2 = W_1 \frac{1}{k_2} + e^{-\mu_1 t}\left(B_1 \cos \nu_1 t + B_2 \sin \nu_1 t\right) +$$

$$e^{-\mu_2 t}\left(B_3 \cos \nu_2 t + B_4 \sin \nu_2 t\right) \qquad (12b)$$

Here μ and ν are obtained from the real and imaginary parts of the four solutions

$$\lambda = -\mu_1 \pm i\nu_1$$

$$\lambda = -\mu_2 \pm i\nu_2$$

of the frequency equation

$$\lambda^4 + \left(\frac{1}{m_1} + \frac{1}{m_2}\right)b\lambda^3 + \left(\frac{k_1}{m_1} + \frac{k_1 + k_2}{m_2}\right)\lambda^2 + \frac{bk_2}{m_1 m_2}\lambda + \frac{k_1 k_2}{m_1 m_2} = 0 \qquad (13)$$

and the B's depend on the A's by the relations

$$\left.\begin{aligned}
B_1 &= \left(1 + \alpha_1\right)A_1 + \beta_1 A_2 \\[2mm]
B_2 &= -\beta_1 A_1 + \left(1 + \alpha_1\right)A_2 \\[2mm]
B_3 &= \left(1 + \alpha_2\right)A_3 + \beta_2 A_4 \\[2mm]
B_4 &= -\beta_2 A_3 + \left(1 + \alpha_2\right)A_4
\end{aligned}\right\} \qquad (14)$$

with

$$\left.\begin{aligned}
\alpha_n &= m_1 \frac{\mu_n^2\left(k_1 - b\mu_n\right) - \nu_n^2\left(k_1 + b\mu_n\right)}{\left(k_1 - b\mu_n\right)^2 + b^2\nu_n^2} \\[4mm]
\beta_n &= m_1 \frac{b\nu_n\left(\mu_n^2 + \nu_n^2\right) - 2k_1\mu_n\nu_n}{\left(k_1 - b\mu_n\right)^2 + b^2\nu_n^2} \qquad n = 1,2
\end{aligned}\right\} \qquad (15)$$

All these formulas are established in the same way as are the corresponding formulas for $m_2 = 0$. It may happen that one pair of λ's is real (or even both pairs). The formulas will then undergo similar changes, like those explained for the third-order problem.

When solution (12) is introduced into the initial conditions (equations (11)) the following equations for A_1 to A_4 will result:

$$A_1 + A_3 = -W_1\left(\frac{1}{k_1} + \frac{1}{k_2}\right)$$

$$-\mu_1 A_1 + \nu_1 A_2 - \mu_2 A_3 + \nu_2 A_4 = V$$

$$\left(\mu_1^2 - \nu_1^2\right)A_1 - 2\mu_1\nu_1 A_2 + \left(\mu_2^2 - \nu_2^2\right)A_3 - 2\mu_2\nu_2 A_4 = \frac{W_1}{m_1}$$

$$\mu_1\left(\mu_1^2 - 3\nu_1^2\right)A_1 - \nu_1\left(3\mu_1^2 - \nu_1^2\right)A_2 + \mu_2\left(\mu_2^2 - 3\nu_2^2\right)A_3 - \nu_2\left(3\mu_2^2 - \nu_2^2\right)A_4 = \frac{bW_1}{m_1^2}$$

$$(16)$$

This set must be solved numerically and then one may find B_1 to B_4 from equations (14) and (15). The stroke $x = x_1 - x_2$ of the shock strut is then:

$$x = \frac{W_1}{k_1} - e^{-\mu_1 t}\left[\left(\alpha_1 A_1 + \beta_1 A_2\right)\cos \nu_1 t - \left(\beta_1 A_1 - \alpha_1 A_2\right)\sin \nu_1 t\right] -$$

$$e^{-\mu_2 t}\left[\left(\alpha_2 A_3 + \beta_2 A_4\right)\cos \nu_2 t - \left(\beta_2 A_3 - \alpha_2 A_4\right)\sin \nu_2 t\right]$$

$$(17a)$$

The force acting between the tire and the ground is again

$$F_2 = k_2 x_2$$

and may be computed from equation (12b). It is responsible for the stresses in the tire, and when it becomes zero the airplane will rebound. But F_2 is not equal to the shock-strut force F_1 which in turn is responsible for the action of this part of the landing gear and for the dynamic load on the airplane structure. This force must be found from equation (1b):

$$F_1 = W_1 + e^{-\mu_1 t}\left\{\left[\left(b\mu_1 - k_1\right)\left(\alpha_1 A_1 + \beta_1 A_2\right) + b\nu_1\left(\beta_1 A_1 - \alpha_1 A_2\right)\right]\cos\nu_1 t + \right.$$

$$\left. \left[b\nu_1\left(\alpha_1 A_1 + \beta_1 A_2\right) - \left(b\mu_1 - k_1\right)\left(\beta_1 A_1 - \alpha_1 A_2\right)\right]\sin\nu_1 t\right\} +$$

$$e^{-\mu_2 t}\left\{\left[\left(b\mu_2 - k_1\right)\left(\alpha_2 A_3 + \beta_2 A_4\right) + b\nu_2\left(\beta_2 A_3 - \alpha_2 A_4\right)\right]\cos\nu_2 t + \right.$$

$$\left. \left[b\nu_2\left(\alpha_2 A_3 + \beta_2 A_4\right) - \left(b\mu_2 - k_1\right)\left(\beta_2 A_3 - \alpha_2 A_4\right)\right]\sin\nu_2 t\right\} \qquad (17b)$$

From the formulas shown here it is clear that the final result is connected with the data of the problem through an algebraic equation of the fourth degree and through a set of four linear equations. Solutions must be obtained numerically for a given set of data, so it is not possible to discuss the features of the solution in general terms. To find out how they look, a series of systematically chosen examples has been computed which will be discussed in the section "Discussion of Numerical Results."

Undamped System

As a basis for this discussion, it is useful to consider the case when the damping b is zero and, additionally, $m_1 \gg m_2$. The second assumption is certainly good but, if used alone, it would not give any substantial mathematical relief. The first assumption is, of course,

not very realistic in a landing gear whose essential purpose is damping, but the conclusions derived will help in understanding the more realistic cases.

When $b = 0$, the frequency equation (equation (13)) loses the terms with λ^3 and λ and, when it is assumed that $m_1 \gg m_2$, the first part of the coefficient of λ^2 may be neglected.

The equation reads then

$$\lambda^4 + \frac{k_1 + k_2}{m_2} \lambda^2 + \frac{k_1 k_2}{m_1 m_2} = 0$$

and its solutions are purely imaginary, say

$$\lambda = \pm i \nu_1$$

and

$$\lambda = \pm i \nu_2$$

When the equation for λ^2 is solved and everywhere $1/m_1$ is neglected against $1/m_2$, it follows that

$$\lambda^2 = -\frac{k_1 + k_2}{2m_2} \pm \frac{k_1 + k_2}{2m_2}$$

The upper sign yields $\lambda^2 = 0$ and hence $\nu_1 = 0$; the lower sign yields

$$\nu_2 = \sqrt{\frac{k_1 + k_2}{m_2}}$$

This indicates that $\nu_1 \ll \nu_2$, but evidently too many small terms were neglected to find a reasonable value for ν_1. It may be obtained from the fact that the third term in the equation must equal $\nu_1^2 \nu_2^2$:

$$\nu_1^2 = \frac{k_1 k_2}{m_1 m_2 \nu_2^2}$$

$$v_1 = \sqrt{\frac{k_1 k_2}{m_1(k_1 + k_2)}}$$

This is indeed much smaller than v_2.

Since $\mu_1 = \mu_2 = 0$, solution (12) loses the damping factors $e^{-\mu t}$ and becomes:

$$x_1 = W_1 \frac{k_1 + k_2}{k_1 k_2} + A_1 \cos v_1 t + A_2 \sin v_1 t + A_3 \cos v_2 t + A_4 \sin v_2 t$$

$$x_2 = W_1 \frac{1}{k_2} + B_1 \cos v_1 t + B_2 \sin v_1 t + B_3 \cos v_2 t + B_4 \sin v_2 t$$

When this expression for x_1 is introduced in initial conditions (11), a very simple set of equations is obtained:

$$\left.\begin{aligned}
A_1 + A_3 &= -W_1\left(\frac{1}{k_1} + \frac{1}{k_2}\right) \\[2mm]
v_1 A_2 + v_2 A_4 &= V \\[2mm]
v_1{}^2 A_1 + v_2{}^2 A_3 &= -\frac{W_1}{m_1} \\[2mm]
v_1{}^3 A_2 + v_2{}^3 A_4 &= 0
\end{aligned}\right\} \tag{18}$$

It consists of two independent pairs which will be solved and discussed separately.

From the first and third equations:

$$A_1 = \frac{W_1}{\nu_2{}^2 - \nu_1{}^2}\left(\frac{1}{m_1} - \nu_2{}^2\,\frac{k_1 + k_2}{k_1 k_2}\right)$$

$$\approx \frac{W_1}{k_1 + k_2}\,\frac{m_2}{m_1}\left[1 - \frac{m_1}{m_2}\,\frac{(k_1 + k_2)^2}{k_1 k_2}\right]$$

$$\approx -W_1\,\frac{k_1 + k_2}{k_1 k_2}$$

$$A_3 = -\frac{W_1}{\nu_2{}^2 - \nu_1{}^2}\left(\frac{1}{m_1} - \nu_1{}^2\,\frac{k_1 + k_2}{k_1 k_2}\right)$$

$$\approx -\frac{W_1}{k_1 + k_2}\,\frac{m_2}{m_1}(1 - 1)$$

$$= 0$$

Equations (15) yield $\beta_1 = \beta_2 = 0$ and

$$\alpha_n = -\frac{m_1}{k_1} - \nu_n{}^2 \qquad\qquad n = 1,\ 2$$

and equations (14),

$$B_1 = A_1\left(1 - \nu_1{}^2\,\frac{m_1}{k_1}\right)$$

$$= -W_1/k_2$$

$$B_3 = A_3\left(1 - \nu_2{}^2\,\frac{m_1}{k_1}\right)$$

$$= 0$$

The last equation is not very convincing as it stands, since it gives B_3 as a product of A_3, which is almost zero, and of the large factor m_1/m_2. But one may check the result by first finding an exact expression for B_3 and then neglecting m_2 against m_1.

From the results it is seen that only the low-frequency motion $\left(A_1, B_1\right)$ is of importance and that the ratio x_2: x_1 is at all times the same as for the static deflections, uninfluenced by the presence of the unsprung mass.

The second and fourth of equations (18) may be handled in the same way. The result is this:

$$A_2 = V\left(\frac{m_1}{k_1 + k_2}\right)^{1/2} \frac{k_1 + k_2}{\left(k_1 k_2\right)^{1/2}}$$

$$A_4 = -V\left(\frac{m_2}{m_1}\right)^{3/2}\left(\frac{m_1}{k_1 + k_2}\right)^{1/2} \frac{k_1 k_2}{\left(k_1 + k_2\right)^2}$$

$$B_2 = V\left(\frac{m_1}{k_1 + k_2}\right)^{1/2}\left(\frac{k_1}{k_2}\right)^{1/2}$$

$$B_4 = V\left(\frac{m_2}{m_1}\right)^{1/2}\left(\frac{m_1}{k_1 + k_2}\right)^{1/2} \frac{k_2}{k_1 + k_2}$$

Here again it is seen that for x_1 the low-frequency motion $\left(A_2\right)$ is by far preponderant, A_4 being smaller by a factor $\left(m_2/m_1\right)^{3/2}$; but for the displacement of the wheel $\left(B_2, B_4\right)$ the factor is only $\left(m_2/m_1\right)^{1/2}$. In the low-frequency motion the ratio x_2: x_1 is the same as for the static deflection, but in the high-frequency motion x_2 is much larger than x_1, the wheel moving up and down between the ground and the almost unmovable airplane mass.

On the whole this analysis shows that through the presence of an "unsprung mass" a high-frequency motion is added to the low-frequency motion of the airplane. This high-frequency motion does not affect x_1,

but it makes a certain contribution to the forces in the shock strut and in the tire. Since $(m_2/m_1)^{1/2}$ is still as small as 0.15, one may neglect the presence of the mass m_2 if the accuracy requirements are not too high. In view of the many arbitrary assumptions which enter the analysis (e.g., the value of V), one may think of neglecting m_2 for design purposes, but one should keep an eye on it when evaluating tests. This rule, of course, is derived from the behavior of the undamped shock strut. How far it is modified by the damping can be seen only from the systematic numerical work which will now be discussed.

Discussion of Numerical Results

Dimensionless parameters.- The formulas developed in the preceding sections have been used to compute some typical examples. In order to draw maximum information from this work, it has been done in dimensionless form, and therefore the choice made for the dimensionless quantities must be discussed before the results may be discussed.

For the displacements x_1 and x_2 and the stroke x a reference length is needed, and when they are plotted against time a reference time is needed. Since the deflections start from zero at $t = 0$ and approach asymptotically definite values, the static deflections, it seems reasonable to adopt the static deflection of the mass m_1 as a standard of length:

$$\delta = m_1 g\left(\frac{1}{k_1} + \frac{1}{k_2}\right)$$

A simple time standard may be found in the period of the vibrations which the mass m_1 can make on the springs k_1 and k_2 in the absence of damping. This period is $2\pi\sqrt{\delta/g}$; drop the factor 2π and choose as time standard

$$T = \sqrt{\frac{\delta}{g}} = \sqrt{\frac{m_1(k_1 + k_2)}{k_1 k_2}}$$

For the forces F_1 and F_2 the load W_1 might be used as standard; but, since W_1 depends on the horizontal speed of the airplane and on the angle of attack of its wings, it may have rather different values for different landing cases of the same airplane. It is therefore better to use $m_1 g$ as a reference value.

Besides these variables there is a set of constants which influence the impact. They are the masses m_1 and m_2, the spring constants k_1 and k_2, the damping b of the shock strut, the load W_1 (weight minus lift), and the vertical velocity V of the airplane. These constants may be combined to the following dimensionless parameters: m_2/m_1, $\frac{k_1}{k_1 + k_2}$, bT/m_1, W_1/m_1g, and VT/δ. These parameters must be chosen for each example.

Influence of unsprung mass.- Of most interest in a study of the linear spring-damper system is the influence of the unsprung mass on the impact force. Since this influence is small in the undamped system, one may hope to find the same result when damping is present. To check whether this is true, a landing gear has been investigated analytically for two extreme values of the mass parameter, $m_2/m_1 = 0$ and $m_2/m_1 = 0.050$. Values common in current practice lie approximately halfway between, and the choice has been made in order to make the effects more clearly visible. For the other parameters the following values were chosen:

$$\frac{k_1}{k_1 + k_2} = 0.25$$

$$bT/m_1 = 0.5$$

$$W_1/m_1g = 0.2$$

$$VT/\delta = 2.0$$

The weight parameter lies halfway between a fully buffered landing with $W_1 = 0$ and the usual assumption of $W_1 = \frac{1}{3} m_1g$. The other three figures are so chosen that they correspond to an actual airplane, at least so far as a correspondence between a linear and a real shock strut is possible.

The result of the computations is seen in figure 3(a) which shows the shock-strut force F_1 against time t. At the start there is a definite difference: The unsprung mass absorbs the first impact and the shock-strut force develops slowly; a slight overshoot follows; and then the

curves are practically parallel, the distance between them corresponding to the addition of the wheel mass m_2 to the total mass $m_1 + m_2$ which must be decelerated.

This result confirms the view that the maximum of the shock-strut force is not much influenced by the unsprung mass and that one may safely assume $m_2 = 0$ when this leads to a simplification of the theoretical or numerical work. However, this simplification may not be admissible when the wheel spin-up must be considered. Figure 3(b) shows the force F_2 between the wheel and the ground, and here it appears that in the early stage there is a considerable difference between the two cases such that F_2 and hence the drag load will increase with the unsprung mass.

Influence of damping.- High damping in the shock strut is desirable since it dissipates the kinetic energy of the airplane and thus prevents repeated rebounding. The influence of damping on the landing impact may be seen in figure 4. Here the force F_2 on the wheel and the stroke x of the shock strut are plotted against time for the following set of parameters:

$$m_2/m_1 = 0.025$$

$$\frac{k_1}{k_1 + k_2} = 0.25$$

$$W_1/m_1 g = 0.2$$

$$VT/\delta = 2.0$$

and $bT/m_1 = 0.5$ and 1.0. In the initial stage there is not much difference between the two curves (fig. 4(a)), since the impact is caught by the tire, but then the rise of F_2 is much faster for the case of higher damping; the maximum is reached more quickly but it is only 7 percent higher than that for the case with half as much damping. The development of the stroke (fig. 4(b)) is on the whole similar in both cases, but the maximum is lower for high damping. The figures show that, apart from its influence on rebounding (which occurs much later), high damping has its pros and cons and that they must be balanced in each design.

Influence of spring constants.- In another example the influence of the spring constants k_1 and k_2 is compared. The forces F_1 and F_2 have been computed for

$$m_2/m_1 = 0.025$$

$$bT/m_1 = 0.5$$

$$W_1/m_1 g = 0.2$$

$$VT/\delta = 2.0$$

and for $\dfrac{k_1}{k_1 + k_2} = 0.15$ and 0.25.

The standards of length and time, δ and T, will not be changed if the sum of the reciprocals $1/k_1 + 1/k_2$ is kept constant, and under this condition an increase of the parameter $k_1/(k_1 + k_2)$ simply means that the shock strut is made stiffer and the tire softer. Consequently, a greater part of the total deformation will take place in the tire, and since there is no damping the impact force will build up more slowly. This is clearly seen in figures 5(a) and 5(b), which show that the influence is the strongest on F_2. Of course, the smaller the impact force, the less the airplane will be decelerated and the higher the force must rise at a later stage to bring the vertical motion to a stop. This is also seen in the diagrams, and in figure 5(c) one sees the consequences for the displacement x_1 of the airplane and the deformation x_2 of the tire.

Influence of weight and lift.- Remember that the notation W_1 represents the resultant static load on the landing gear, essentially the difference of the weight of the airplane and the wing lift. In the landing-gear literature one finds discussions of the whole gamut of possibilities from the buffered landing with $W_1 = 0$ to the pancake landing $W_1 = m_1 g$. The present American regulations consider $W/m_1 g = 0.333$ as a standard assumption. The cases where $W_1/m_1 g = 0$ and 0.2 have been computed, assuming

$$m_2/m_1 = 0$$

$$\frac{k_1}{k_1 + k_2} = 0.25$$

$$bT/m_1 = 0.5$$

$$VT/\delta = 2.0$$

The corresponding forces $F_2 = F_1$ are shown in figure 6, and one recognizes that the difference is not very pronounced. This is easily understood when one considers the maximum displacement x_1 of the airplane mass. It is 1.65δ in the first case and 1.82δ in the second, while the final static deflections will be 0 and 0.2δ, respectively. It is therefore essentially the kinetic energy of the airplane mass and not the weight that is responsible for the impact.

All the examples given here show the general trend of changes which a change of one of the parameters will induce. In the details much will be different when real shock struts with their essential nonlinearity are considered.

Taxying

When an airplane taxies on the ground, its tires and the shock struts have the same functions as the tires and springs of an automobile. Whether they will be subject to serious dynamic forces depends on the smoothness of the ground. In the investigation of the taxying impact it has become customary to assume that the airplane rolls at moderate speed over a bump shaped after a sine curve. On a turf-covered airfield such a bump may represent a frozen molehill or a similar obstacle, but on a well-kept concrete runway it is difficult to discover an obstacle of this kind from which the length and height of the bump might be taken, and the same is true for the deck of an aircraft carrier.

It is preferred therefore to assume as a standard obstacle a step in the ground, as it is encountered in the joints between the runway slabs or if a wheel should get over the edge of the pavement (fig. 7).

For the mathematical formulation of the problem it is assumed that the airplane is taxying on the left part of the pavement and that the landing gear has the static deflection:

$$x_1 = W_1 \frac{k_1 + k_2}{k_1 k_2}$$

$$x_2 = W_1 \frac{1}{k_2}$$

Since taxying is done at low speed, W_1 in these formulas comes close to the total weight $m_1 g$ to be carried by one shock strut.

At $t = 0$ the wheel hits the step in the pavement, and for $t > 0$ the term $k_2 x_2$ in equation (2b), which represents the force in the tire, must be replaced by $k_2(x_2 + h)$. The equilibrium is then disturbed, and it is desired to know the resulting vibration. It will be found by solving the differential equations

$$m_1 \ddot{x}_1 + b\left(\dot{x}_1 - \dot{x}_2\right) + k_1\left(x_1 - x_2\right) = W_1 \tag{19a}$$

$$m_2 \ddot{x}_2 - b\left(\dot{x}_1 - \dot{x}_2\right) - k_1\left(x_1 - x_2\right) + k_2 x_2 = -k_2 h \tag{19b}$$

for the following set of initial conditions:

$$t = 0: \qquad x_1 = W_1 \frac{k_1 + k_2}{k_1 k_2}, \qquad x_2 = W_1 \frac{1}{k_2}, \qquad \dot{x}_1 = \dot{x}_2 = 0$$

It will again be useful to write all initial conditions in terms of one variable. Since it will be seen that in the present case x_2 is more important than x_1, x_2 is chosen to formulate the conditions. The procedure is almost the same as that described in the section "Solution Not Neglecting Unsprung Mass," and the result is this:

$$t = 0: \qquad x_2 = W_1 \frac{1}{k_2}, \qquad \dot{x}_2 = 0, \qquad \ddot{x}_2 = -\frac{k_2 h}{m_2}, \qquad \dddot{x}_2 = \frac{b k_2 h}{m_2^2} \tag{20}$$

The solution of equations (19) has, of course, almost the form of equations (12). Because of the new term on the right-hand side of equation (19b) it is:

$$x_1 = W_1 \frac{k_1 + k_2}{k_1 k_2} - h + e^{-\mu_1 t}\left(A_1 \cos \nu_1 t + A_2 \sin \nu_1 t\right) + e^{-\mu_2 t}\left(A_3 \cos \nu_2 t + A_4 \sin \nu_2 t\right) \qquad (21a)$$

$$x_2 = W_1 \frac{1}{k_2} - h + e^{-\mu_1 t}\left(B_1 \cos \nu_1 t + B_2 \sin \nu_1 t\right) + e^{-\mu_2 t}\left(B_3 \cos \nu_2 t + B_4 \sin \nu_2 t\right) \qquad (21b)$$

When this is introduced into the initial conditions, equations (20), the following set of equations for B_1 to B_4 will result:

$$\left.\begin{array}{l} B_1 + B_3 = h \\[2ex] \mu_1 B_1 - \nu_1 B_2 + \mu_2 B_3 - \nu_2 B_4 = 0 \\[2ex] \left(\mu_1{}^2 - \nu_1{}^2\right)B_1 - 2\mu_1\nu_1 B_2 + \left(\mu_2{}^2 - \nu_2{}^2\right)B_3 - 2\mu_2\nu_2 B_4 = -\frac{k_2 h}{m_2} \\[2ex] \mu_1\left(\mu_1{}^2 - 3\nu_1{}^2\right)B_1 - \nu_1\left(3\mu_1{}^2 - \nu_1{}^2\right)B_2 + \mu_2\left(\mu_2{}^2 - 3\nu_2{}^2\right)B_3 - \nu_2\left(3\mu_2{}^2 - \nu_2{}^2\right)B_4 = -\frac{b k_2 h}{m_2{}^2} \end{array}\right\} \qquad (22)$$

When these equations have been solved, the constants A must be computed. This is done by inverting equations (14):

$$A_1 = \frac{\left(1 + \alpha_1\right)B_1 - \beta_1 B_2}{\left(1 + \alpha_1\right)^2 + \beta_1{}^2}$$

$$A_2 = \frac{\beta_1 B_1 + \left(1 + \alpha_1\right)B_2}{\left(1 + \alpha_1\right)^2 + \beta_1^{\ 2}}$$

$$A_3 = \frac{\left(1 + \alpha_2\right)B_3 - \beta_2 B_4}{\left(1 + \alpha_2\right)^2 + \beta_2^{\ 2}}$$

$$A_4 = \frac{\beta_2 B_3 + \left(1 + \alpha_2\right)B_4}{\left(1 + \alpha_2\right)^2 + \beta_2^{\ 2}}$$

Now x_1 and x_2 and their derivatives may be calculated as functions of time and from them, the stroke $x = x_1 - x_2$, the force on the wheel $F_2 = k_2\left(x_2 + h\right)$, and the force in the shock strut

$$F_1 = W_1 - m_1 \ddot{x}_1$$

$$= W_1 - m_1 e^{-\mu_1 t} \left\{ \left[\left(\mu_1^{\ 2} - \nu_1^{\ 2}\right)A_1 - 2\mu_1 \nu_1 A_2\right] \cos \nu_1 t + \right.$$

$$\left. \left[2\mu_1 \nu_1 A_1 + \left(\mu_1^{\ 2} - \nu_1^{\ 2}\right)A_2\right] \sin \nu_1 t \right\} -$$

$$m_1 e^{-\mu_2 t} \left\{ \left[\left(\mu_2^{\ 2} - \nu_2^{\ 2}\right)A_3 - 2\mu_2 \nu_2 A_4\right] \cos \nu_2 t + \right.$$

$$\left. \left[2\mu_2 \nu_2 A_3 + \left(\mu_2^{\ 2} - \nu_2^{\ 2}\right)A_4\right] \sin \nu_2 t \right\}$$

An example may illustrate the mechanical content of these formulas. The following set of dimensionless data is chosen:

$$m_2/m_1 = 0.025$$

$$\frac{k_1}{k_1 + k_2} = 0.15$$

$$bT/m_1 = 0.5$$

$$W_1/m_1 g = 1$$

$$h/\delta = 0.1$$

After solving frequency equation (13) one may find B_1 to B_4 from set (22):

$$B_1 = 0.0137\delta$$

$$B_2 = 0.011\delta$$

$$B_3 = 0.0863\delta$$

$$B_4 = 0.0617\delta$$

The precision of B_2 is rather poor, but it is not possible to obtain a more accurate value unless the data of the problem are given with such accuracy that a computation with more than slide-rule accuracy would be justified. However, B_2 is multiplied in equation (21b) with a factor which increases rather slowly with t, and the term does not reach an important magnitude before the essential phase of the impact is passed. The displacement x_2 of the wheel is shown by the solid line in figure 8. The displacement x_1 of the airplane has not been plotted because it is almost constant, and only after a considerably longer lapse of time does the airplane climb slowly to the new level given by the step in the runway.

The forces F_1 in the shock strut and F_2 in the tire are
represented by the solid lines in figure 9. The force F_2 jumps
instantaneously from its static value $F_2 = W_1$ to $1.67W_1$, the rise
being determined by the height h of the step and by the stiffness k_2
of the tire. Actually this sudden increase of F_2 is smoothened by
local deformation of the tire. The force F_1 which through the shock
strut acts on the airplane structure rises smoothly to a maximum and
then returns in damped oscillations to its static value W_1. In the
present example the essential part of the impact is passed at $t = 0.15T$.

The fact that the mass m_1 hardly moves within that time which is
of interest suggests simplifying the computations by putting $m_1 = \infty$.
When this is done, equation (19a) must be dropped entirely (it simply
yields $\ddot{x}_1 = 0$) and in equation (19b) there must be put

$$x_1 = \delta = W_1 \frac{k_1 + k_2}{k_1 k_2}$$

$$\dot{x}_1 = 0$$

The problem is then reduced from the fourth to the second order and its
solution is

$$x_2 = \frac{W_1}{k_2} - \frac{k_2 h}{k_1 + k_2} + e^{-\mu t}\left(B_1 \cos \nu t + B_2 \sin \nu t\right)$$

with

$$\mu = \frac{b}{2m_2}$$

$$\nu = \frac{1}{2m_2} \sqrt{4\left(k_1 + k_2\right)m_2 - b^2}$$

Of the initial conditions (equations (20)) only the first two remain
valid, and from them

$$B_1 = \frac{k_2 h}{k_1 + k_2}$$

$$B_2 = \frac{\mu}{\nu} B_1$$

With these formulas it is rather easy to compute the deflection x_2 and the forces

$$F_1 = k_1 \left(x_1 - x_2 \right) + b \left(\dot{x}_1 - \dot{x}_2 \right)$$

$$= W_1 \frac{k_1 + k_2}{k_2} - k_1 x_2 - b \dot{x}_2$$

$$= W_1 + \frac{k_1 k_2 h}{k_1 + k_2} - e^{-\mu t} \left[\left(k_1 B_1 - b\mu B_1 + b\nu B_2 \right) \cos \nu t + \right.$$

$$\left. \left(k_1 B_2 - b\nu B_1 - b\mu B_2 \right) \sin \nu t \right]$$

$$F_2 = k_2 x_2$$

However, there is still a difficulty in the dimensionless representation of the results. When m_1 is put equal to ∞, the quantity which was used as a reference basis for m_2, bT, and W_1 seems to be lost. But this difficulty is only apparent. When m_1 is set equal to ∞ in an equation, this does not mean that the mass really is infinite but only that the inertia is intentionally overrated. Nevertheless, there is a certain weight $m_1 g$ to which the load (weight minus lift) W_1 and the weight $m_2 g$ of the wheel may be referred and which will produce a

certain static deflection δ. To this deflection the height h of the step is referred, and the damping b is handled by writing

$$\frac{bT}{m_1} = \frac{b}{m_1} \sqrt{\delta/g}$$

$$= \frac{b}{m_1 g} \sqrt{\delta g}$$

With this interpretation of the dimensionless quantities, the results of the simplified theory may be plotted in the same diagrams which were used before. They are represented by the broken lines in figures 8 and 9.

These curves show the following features: (1) In the domain of interest they are so close to the exact curves that they can hardly be distinguished. (2) For large values of t they have different asymptotes. This is easily explained. When x_1 = Constant, the springs will find themselves at last more compressed than they were before the impact. The wheel can therefore not rise by the full height h of the step, and the forces $F_1 = F_2$ will be higher than W_1. However, this deviation between the two solutions is of no practical importance, not so much because of its small magnitude but because of its late occurrence.

It is of some interest to study the extreme case that $m_1 = \infty$ and $m_2 = 0$. Since the mass m_2 is responsible for the difference between the forces F_1 and F_2, it is seen from a glance at figure 9 that this simplification of the problem goes too far to yield results of immediate practical value. The formulas therefore will not be reproduced, but some points computed from them have been entered in the force diagram (fig. 9). This line of dots which represent both F_1 and F_2 shows approximately how the solution will be changed if the unsprung mass m_2 is substantially decreased: The sudden rise of F_2 is the same, but the following decrease is faster. The force F_1 rises more rapidly (in the limiting case has the same discontinuous increase as F_2), and its maximum will be higher the more m_2 is decreased. This shows that in taxying it is not advantageous to have the unsprung mass too small.

INTENTIONAL NONLINEARITIES

The kind of shock strut considered in the section "Linear Spring-Damper Systems" is the only one which leads to linear differential equations. The spring terms in these equations correspond to the action of helical or other steel springs, and such springs were used to some extent in early shock struts. Modern shock struts use air as an elastic material, and air does not show linear elasticity unless there is time enough to dissipate the heat generated by compression. However, the nonlinearity introduced by a pneumatic spring is not severe, even in the extreme case of adiabatic compression.

Quite different is the situation with the damping term in equation (1b). Viscous damping is never realized in shock struts, their damping being produced by the acceleration of oil squeezed through narrow orifices or slots. If the cross section of the orifice does not vary, one has a velocity-square damping, and this already presents an essential nonlinearity. But more than this, the necessity of making the best use of the structural weight of the landing gear has led to the introduction of a metering pin which changes the width of the orifice in such a way as to make the impact force increase quickly to its peak value and then stay at this value for a considerable time. The nonlinearity which the metering pin introduces into the differential equations is intentional and essential, and one has to study the equations of motion with the corresponding damping term. This will be done in this part of the report and, since there is no additional difficulty connected with it, the nonlinear elasticity of the air spring will also be included.

Differential Equation of Oleo Strut

Oleo struts are built in different forms (fig. 10). They all have this in common: A piston moves in a cylinder, and there are two chambers, separated by a diaphragm and connected by an orifice. The lower chamber is filled with oil; the upper one, partly with oil and partly with air. When the strut is compressed, oil must flow from the lower to the upper chamber, and there may or may not be a metering pin which fills part of the orifice and makes the remaining gap depend on the position of the piston.

The pressure p_1 in the upper chamber depends only on the air volume and hence on the position of the piston. The pressure p_2 in the lower chamber is greater by the pressure which is needed to squeeze oil through the orifice. The difference is proportional to the square of the piston velocity and thus produces a damping of the shock-strut motion.

The relation between the force F_1 transmitted through the shock strut, the stroke x, and the rate of stroke $\dot{x}$ will now be established. In addition to the notations explained in figures 10(a) and 10(b), the following symbols for the different cross-sectional areas are used:

A_0 inner cross section of barrel at oil level

A_1 total cross section of piston

A_2 inner cross section of piston in figure 10(b)

When the strut is fully expanded and at rest, there will be a certain pressure p_0 in both chambers and a force up to the limit

$$F_0 = p_0 A_1$$

may be applied without displacing the piston.

When the piston is displaced, the content of the chambers is decreased by $x A_1$ and, since the oil is incompressible, the air volume must decrease by this amount:

$$x A_1 = (z_0 - z) A_0$$

The collapse of a shock strut under the landing impact takes less than 1 second, and one might think that this time would be too short to allow for much heat transfer. Then the compression of the air would follow the adiabatic law

$$p_1 z^{\gamma} = p_0 z_0^{\gamma}$$

with $\gamma = 1.4$. There is, however, a very efficient cooling of the air through the jet of cool oil which is shot vigorously through the orifice and scattered on the cylinder walls. It may therefore be justified to assume a much lower value for the exponent, say $\gamma = 1.1$ or even isothermal compression with $\gamma = 1$. To decide this point, temperature measurements in the air chamber would be needed.

Elimination of z from the last two equations yields the following expression for the pressure in the upper chamber:

$$p_1 = p_0 \left(\frac{z_0 A_0 / A_1}{z_0 A_0 / A_1 - x} \right)^\gamma \qquad (23)$$

When the piston is displaced, the volume of the lower chamber is decreased and oil must flow through the orifice into the upper chamber. In the case of figure 10(a) the rate of the oil flow is $A_1\dot{x}$; in the case of figure 10(b) it is $A_2\dot{x}$, and the oil velocity in the orifice is

$$v = \frac{A_1\dot{x}}{A_3}$$

or

$$v = \frac{A_2\dot{x}}{A_3}$$

Here A_3 represents essentially the area of the gap between the metering pin and the edge of the orifice, inclusive of an orifice coefficient, if necessary. This gap area depends in a known way on the stroke x. But A_3 includes also any other leakage between the two chambers, and such additional gaps may depend on elastic deformations and hence on the pressure p_2. Complications are avoided by disregarding this fact and assuming that A_3 is known or sufficiently estimated as a function of x alone.

The oil is accelerated to the velocity v by the difference between the pressures p_2 and p_1 in the two chambers according to Bernoulli's equation

$$p_2 - p_1 = \frac{1}{2}\rho v^2$$

where ρ is the density (mass per unit volume) of the oil. Taking the last two equations together, a relation is obtained between the pressures and $\dot{x}$:

$$p_2 - p_1 = \frac{\rho A_1^2}{2A_3^2} \dot{x}^2$$

or

$$p_2 - p_1 = \frac{\rho A_2^2}{2A_3^2} \dot{x}^2$$

(24)

respectively, for figures 10(a) and 10(b).

In this form, the relation holds only for the upward stroke. During the recoil motion of the piston the oil moves in the opposite direction through the orifice and the pressure in the upper chamber is the higher one. To cover this motion, one must at least write $p_1 - p_2$ instead of $p_2 - p_1$ in equations (24). However, even this will not really describe the recoil motion, for the following reason: The oil jet which is shot in the upper chamber during the upstroke is so vigorous that air and oil get thoroughly mixed, and this foam is squeezed back during the downstroke. It is therefore scarcely possible to calculate the details of the downstroke until experimental information becomes available concerning the degree of mixing and the density ρ which should be used in equations (24) for this phase of the motion.

In figure 10(a) the force acting downward on the piston is simply

$$F_1 = A_1 p_2$$

$$= A_1 p_1 + A_1 (p_2 - p_1)$$

In figure 10(b) part of the piston protrudes into the upper chamber and is there exposed to the pressure p_1. The total force is therefore in this case

$$F_1 = (A_1 - A_2) p_1 + A_2 p_2$$

$$= A_1 p_1 + A_2 (p_2 - p_1)$$

With equations (23) and (24) this yields for figure 10(b):

$$F_1 = A_1 p_0 \left(\frac{z_0 A_0/A_1}{z_0 A_0/A_1 - x} \right)^{\gamma} + \frac{\rho A_2^{\,3}}{2 A_3^{\,2}} \dot{x}^2 \qquad (25)$$

and for figure 10(a) the relation is the same except that A_2 must be put equal to A_1. Equation (25) is the equation of the oleo-pneumatic shock strut.

For obvious reasons real shock struts differ from the idealized figures 10(a) and 10(b) in that the upper end of the piston is so shaped that it touches the wall of the barrel. In this way a separate annular space is created between the plunger piston and the wall of the barrel which is usually connected by good-sized holes with the upper chamber. The oil flow through these holes may add some damping. It is easily possible to take care of this effect by a correction of the factor of the second term in equation (25).

Dynamic Equations for Landing Impact

For this study it will be assumed that the force in the tire follows a linear law:

$$F_2 = k_2 x_2$$

but that the force F_1 in the shock strut depends nonlinearly on the stroke x and on the rate of stroke $\dot{x}$:

$$F_1 = F_1(\dot{x}, \; x)$$

the function F_1 being given by equation (25).

The equations of motion are essentially the same as equations (2) except that the terms

$$b\left(\dot{x}_1 - \dot{x}_2 \right) + k_1 \left(x_1 - x_2 \right) = b\dot{x} + k_1 x$$

must be replaced by $F_1(\dot{x}, x)$. The equations are therefore these:

$$m_1\ddot{x}_1 + F_1(\dot{x}, x) = W_1 \tag{26a}$$

$$m_2\ddot{x}_2 - F_1(\dot{x}, x) + k_2x_2 = 0 \tag{26b}$$

Since these equations contain three unknown variables, a third equation is needed, the relation

$$x = x_1 - x_2 \tag{26c}$$

The initial conditions for these equations will be different from those used with equations (2). Because of the prestressing of the oleo strut there will be a short but finite time at the beginning of the impact when the piston does not move and the total of the deflection comes from the tire. During this interval the motion is governed by the differential equation

$$\left(m_1 + m_2\right)\ddot{x}_2 + k_2x_2 = W_1$$

and to it the initial conditions

$$t = 0: \qquad x_2 = 0, \qquad \dot{x}_2 = V$$

must be applied. The solution is

$$x_1 = x_2 = \frac{W_1}{k_2}(1 - \cos \omega t) + \frac{V}{\omega} \sin \omega t$$

$$\omega^2 = \frac{k_2}{m_1 + m_2}$$

It is valid up to the time $t = t_0$ when for the first time

$$k_2 x_2 = F_0$$

the prestress force of the shock strut. From

$$\frac{W_1}{k_2}(1 - \cos \omega t_0) + \frac{V}{\omega} \sin \omega t_0 = F_0$$

one finds t_0 and then

$$X_0 = \frac{W_1}{k_2}(1 - \cos \omega t_0) + \frac{V}{\omega} \sin \omega t_0$$

$$V_0 = \frac{W_1 \omega}{k_2} \sin \omega t_0 + V \cos \omega t_0$$

the displacement and velocity at the end of the initial interval. With these quantities the initial conditions for equations (26) may now be written. They are

$$\left. \begin{array}{c} x_1 = x_2 = X_0 \\ \\ \dot{x}_1 = \dot{x}_2 = V_0 \end{array} \right\} \tag{27}$$

These conditions ought to be imposed at $t = t_0$. For the numerical solution it is more convenient to start a new time scale in which equations (27) are to be satisfied at $t = 0$. When plotting the results, one should of course convert the time so that the zero is at the moment of first contact.

Equations (26a) to (26c) with boundary conditions (27) must be solved by a step-by-step integration. As is well-known, this is done in the following way: At a certain time t, the differential equations are used to compute the numerical value of the highest derivative of each unknown; then one of various integration methods is used to find

values of the unknowns themselves for the time $t + \Delta t$. The choice of the integration method determines the exactness of the result and the amount of computation work needed. This point will be discussed in the next section.

The other part of the process, the computation of $\ddot{x}_1$ and $\ddot{x}_2$, is done in table 1.

TABLE 1

(1)	(2)	(3)	(4)	(5)	(6)	(7)	(8)	(9)	(10)	(11)	(12)
t	x_1	$\dot{x}_1$	x_2	$\dot{x}_2$	x	$\dot{x}$	$F_1(x,\ \dot{x})$	$k_2 x_2$	$\ddot{x}_2$	$W_1 - F_1$	$\ddot{x}_1$
0											

In the first line of this table, columns (2) to (5) are filled from the initial conditions. Then columns (6) and (7) are filled with the help of equation (26c) and columns (8) to (10) and (11) and (12), with the help of equations (26b) and (26a). The integration process will then yield values for the second line of columns (2) to (5), and then the whole procedure may be repeated.

Simplified Equations, Neglecting Unsprung Mass

As has been seen before, the unsprung mass does not essentially influence the load-stroke curve. It is therefore of interest to reconsider equations (26a) to (26c) after dropping the term with m_2 :

$$m_1 \ddot{x}_1 = W_1 - F_1 \tag{28a}$$

$$F_1(\dot{x},\ x) = k_2 x_2 \tag{28b}$$

$$x = x_1 - x_2 \tag{28c}$$

As seen already in the linear case, neglecting the unsprung mass decreases the order of the problem by one and the initial condition for $\dot{x}_2$ must be dropped.

Equations (28) may be handled numerically with the help of table 2, combined with a table for the numerical integrations.

TABLE 2

(1)	(2)	(3)	(4)	(5)	(6)	(7)	(8)	(9)	(10)
t	x_1	$\dot{x}_1$	x_2	x	F_1	$\dot{x}$	$\dot{x}_2$	$W_1 - F_1$	$\ddot{x}_1$
0									

Here in the first line columns (2) to (4) are filled from the initial conditions and the other columns, with the help of equations (28c), (28b), and (28a). The first step of the numerical integration serves to get the second line started, and so forth.

Methods of Numerical Integration

There exists much literature on the subject of numerical integrations and it does not seem necessary to develop here new methods or to describe the old ones in detail. But it appears to be useful to recommend methods which have sufficient accuracy without being too laborious, to explain their background, and to present the necessary working formulas in a notation adapted to the present purposes. This will be done here, and for further details the reader is referred to the literature.[1]

The functions which have to be integrated with respect to time are $\ddot{x}_1$, $\dot{x}_1$, $\dot{x}_2$, and, if m_2 is not neglected, $\ddot{x}_2$.

Let $\dot{y}$ be any one of them and assume that, for a certain time $t = t_n$, $\dot{y}_n$ and y_n are known. A first approximation may then be found for the value y_{n+1} of y at $t = t_n + \Delta t$ by assuming that $\dot{y} = \dot{y}_n$ is constant throughout the time interval:

$$y_{n+1} = y_n + \dot{y}_n \, \Delta t \tag{29}$$

---

[1]See, e.g., Scarborough, James B.: Numerical Mathematical Analysis. The Johns Hopkins Press (Baltimore), 1930, p. 227; second ed., 1950, p. 244.

When this value y_{n+1} (in this case values of x_1, $\dot{x}_1$, and x_2) is introduced in the differential equations, $\dot{y}_{n+1}$ is found, and now the integration may be improved by using the average of $\dot{y}_n$ and $\dot{y}_{n+1}$:

$$y_{n+1} = y_n + \frac{1}{2}\left(\dot{y}_n + \dot{y}_{n+1}\right) \Delta t \qquad (30)$$

In figure 11 the first formula uses the shaded rectangle as increment Δy and the second formula uses the shaded trapezoid, but this result is still not final, because with the improved y_{n+1} the differential equation will yield another and better value for $\dot{y}_{n+1}$ which now should be used for the average. The procedure must be repeated until y_{n+1} and $\dot{y}_{n+1}$ no longer change. When the time step Δt is well-chosen, this should occur after the first or second repetition.

An example is shown in tables 3 and 4. Table 3 is identical with table 2 and corresponds to the simplified analysis with $m_2 = 0$. In table 4 there are several consecutive lines for each time t, each of them resulting from one complete cycle of iteration. One sees that $\dot{x}_1$ and x_1 are practically settled after the first cycle and that x_2 required most of the effort. The computation may be speeded up if proper advantage is taken of this situation. One begins the second line of table 4 with the last three columns. With $x_2 = 1.287$ inches and equations (28b) and (28a) the columns F_1, $W_1 - F_1$, and $\dot{x}_1$ of the second line of table 3 may be filled. It is then possible to enter $\ddot{x}_1 = -155.2$ inches per second squared in the second line of table 4 and to perform the two integrations leading to $\dot{x}_1$ and x_1 at once with the trapezoid formula, equation (30). The values so obtained for $\dot{x}_1$ and x_1 will be close to the final ones, and one may now run as many cycles as necessary in the x_2 integration and finally check $\dot{x}_1$ and x_1 again. Great care should be taken that the next step is not started before a perfect result has been obtained, because otherwise avoidable errors would accumulate from step to step in the integration.

TABLE 3

(1) t (sec)	(2) x_1 (in.)	(3) $\dot{x}_1$ (in./sec)	(4) x_2 (in.)	(5) x (in.)	(6) F_1 (lb)	(7) $\dot{x}$ (in./sec)	(8) $\dot{x}_2$ (in./sec)	(9) $W_1 - F_1$ (lb)	(10) $\ddot{x}_1$ (in./sec²)
0	0.988	119.5	0.988	0	12,350	0	119.5	-12,350	-119.2
.0025	1.286	119.2	1.287	0	16,090	15.0	104.2	-16,090	-155.2
.0025	1.286	119.2	1.268	.018	15,850	14.2	105.0	-15,850	-153.0
.0050	1.583	118.8	1.530	.053	19,120	18.6	100.2	-19,120	-184.7
.0050	1.583	118.7	1.524	.059	19,060	18.4	100.3	-19,060	-184.0
.0075	1.879	118.3	1.775	.104	22,200	20.5	97.8	-22,200	-214.2
.0075	1.879	118.2	1.772	.107	22,170	20.3	97.9	-22,170	-214.0
.0100	2.174	117.7	2.017	.157	25,200	21.3	96.4	-25,200	-243.4
.0100	2.174	117.7	2.015	.159	25,200	21.3	96.4	-25,200	-243.4
.	.	.	.	.	.	.	.	.	.
.	.	.	.	.	.	.	.	.	.
.	.	.	.	.	.	.	.	.	.

TABLE 4

(1) t (sec)	(2) $\ddot{x}_1$ (in./sec²)	(3) $\Delta\dot{x}_1$ (in./sec)	(4) $\dot{x}_1$ (in./sec)	(5) Δx_1 (in.)	(6) x_1 (in.)	(7) $\dot{x}_2$ (in./sec)	(8) Δx_2 (in.)	(9) x_2 (in.)
0	-119.2		119.5		0.988	119.5		0.988
		-0.298		0.298			0.299	
.0025	-155.2		119.20		1.286	104.2		1.287
		-.343		.298			.280	
.0025	-153.0		119.16		1.286	105.0		1.268
		-.340		.298			.280	
.0025			119.16		1.286			1.268
		-.382		.297			.262	
.0050	-184.7		118.78		1.583	100.2		1.530
		-.422		.297			.256	
.0050	-184.0		118.74		1.583	100.3		1.524
		-.421		.297			.256	
.0050			118.74		1.583			1.524
		-.460		.296			.251	
.0075	-214.2		118.28		1.879	97.8		1.775
		-.498		.296			.248	
.0075	-214.0		118.24		1.879	97.9		1.772
		-.498		.296			.248	
.0075			118.24		1.879			1.772
		-.535		.295			.245	
.0100	-243.4		117.70		2.174	96.4		2.017
		-.572		.295			.243	
.0100			117.67		2.174			2.015
.	.	.	.	.	.	.	.	.
.	.	.	.	.	.	.	.	.
.	.	.	.	.	.	.	.	.

In practical computation work it is more convenient not to write all the lines shown in tables 3 and 4 but to erase each figure as soon as it can be replaced by a better one. All that is then left of table 4 is shown in table 4(a). As one may see, this table has the great advantage that the figures needed for averaging always stand close together.

TABLE 4(a)

(1)	(2)	(3)	(4)	(5)	(6)	(7)	(8)	(9)
t (sec)	$\ddot{x}_1$ (in./sec²)	$\Delta\dot{x}_1$ (in./sec)	$\dot{x}_1$ (in./sec)	Δx_1 (in.)	x_1 (in.)	$\dot{x}_2$ (in./sec)	Δx_2 (in.)	x_2 (in.)
0	-119.2		119.5		0.988	119.5		0.988
		-0.340		0.298			0.280	
.0025	-153.0		119.16		1.286	105.0		1.268
		-.421		.297			.256	
.0050	-184.0		118.74		1.583	100.3		1.524
		-.498		.296			.248	
.0075	-214.0		118.24		1.879	97.9		1.772
		-.572		.295			.243	
.0100	-243.4		117.67		2.174	96.4		2.015
.	.	.	.	.	.	.	.	.
.	.	.	.	.	.	.	.	.
.	.	.	.	.	.	.	.	.

The procedure may be accelerated considerably if at the start of a new step a good guess is made for the new increment instead of first computing a poor approximation with equation (29). If this is done and if the step Δt is chosen small enough, the method works rapidly and nevertheless develops good accuracy.

Most of the criticism which this method has received in the literature applies only to its use in problems which require a much higher accuracy than does the landing-impact problem. In this case slide-rule accuracy will always be sufficient, and this can be obtained by the trapezoid integration without resorting to painfully small steps.

However, the method has the disadvantage that one never knows exactly how large the error is. This drawback will be avoided if the straight line in figure 11 is replaced by an interpolation parabola. This may be done as soon as four or five successive values of y have been determined.

Through five consecutive points (fig. 12) a parabola of the fourth degree may be fitted, and the coefficients of the corresponding polynomial in t may be written in terms of the ordinates $\dot{y}_{n-4}$, $\dot{y}_{n-3}$, $\cdots$ $\dot{y}_n$ or, better, in terms of $\dot{y}_n$ and of a set of differences of increasing order

$$\Delta_1 \dot{y}_n = \dot{y}_n - \dot{y}_{n-1}$$

$$\Delta_2 \dot{y}_n = \Delta_1 \dot{y}_n - \Delta_1 \dot{y}_{n-1}$$

and so forth which may be computed in the following scheme:

t	$\dot{y}$	$\Delta_1 \dot{y}$	$\Delta_2 \dot{y}$	$\Delta_3 \dot{y}$	$\Delta_4 \dot{y}$
t_{n-4}	$\dot{y}_{n-4}$				
t_{n-3}	$\dot{y}_{n-3}$	$\Delta_1 \dot{y}_{n-3}$			
t_{n-2}	$\dot{y}_{n-2}$	$\Delta_1 \dot{y}_{n-2}$	$\Delta_2 \dot{y}_{n-2}$		
t_{n-1}	$\dot{y}_{n-1}$	$\Delta_1 \dot{y}_{n-1}$	$\Delta_2 \dot{y}_{n-1}$	$\Delta_3 \dot{y}_{n-1}$	
t_n	$\dot{y}_n$	$\Delta_1 \dot{y}_n$	$\Delta_2 \dot{y}_n$	$\Delta_3 \dot{y}_n$	$\Delta_4 \dot{y}_n$

The polynomial may then be integrated over any one of the intervals Δt and in this way improved values for the increments Δy may be obtained. They are computed from the following formulas:

$$\Delta y_n = y_n - y_{n-1}$$
$$= \Delta t \left(\dot{y}_n - \frac{1}{2} \Delta_1 \dot{y}_n - \frac{1}{12} \Delta_2 \dot{y}_n - \frac{1}{24} \Delta_3 \dot{y}_n - \frac{19}{720} \Delta_4 \dot{y}_n \cdots \right) \qquad (31a)$$

$$\Delta y_{n-1} = y_{n-1} - y_{n-2}$$
$$= \Delta t \left(\dot{y}_n - \frac{3}{2} \Delta_1 \dot{y}_n + \frac{5}{12} \Delta_2 \dot{y}_n + \frac{1}{24} \Delta_3 \dot{y}_n + \frac{11}{720} \Delta_4 \dot{y}_n \cdots \right) \qquad (31b)$$

$$\Delta y_{n-2} = y_{n-2} - y_{n-3}$$
$$= \Delta t \left(\dot{y}_n - \frac{5}{2} \Delta_1 \dot{y}_n + \frac{23}{12} \Delta_2 \dot{y}_n - \frac{3}{8} \Delta_3 \dot{y}_n - \frac{19}{720} \Delta_4 \dot{y}_n \cdots \right) \qquad (31c)$$

From these Δy's improved values of the y's are obtained. When they are introduced in the differential equations, better values of the derivatives will be found, and this procedure must be repeated until the results become stationary. This should occur after two or three cycles. If it takes longer this indicates that the time step Δt was chosen too long, and one should at once make a new start with shorter intervals. On the other hand, if the final values are hit at the first stroke, this generally indicates that the time step was chosen too short, and one should start again with a greater Δt or continue until eight lines are completed and then double the step by dropping every other one.

When this polynomial method is applied to the landing-gear problem, columns (1) to (6) of table 4 must be replaced by table 5, and the columns

TABLE 5

(1)	(2)	(3)	(4)	(5)	(6)	(7)	(8)	(9)	(10)	(11)	(12)	(13)	(14)
t	$\ddot{x}_1$	$\Delta_1\ddot{x}_1$	$\Delta_2\ddot{x}_1$	$\Delta_3\ddot{x}_1$	$\Delta_4\ddot{x}_1$	$\Delta\dot{x}_1$	$\dot{x}_1$	$\Delta_1\dot{x}_1$	$\Delta_2\dot{x}_1$	$\Delta_3\dot{x}_1$	$\Delta_4\dot{x}_1$	Δx_1	x_1
-	-						-						-
-	-	.					.	.	.			.	.
-	-	.	.				.	.	.	.		.	.
-	-	.	.	.			.	.	.	.	.	.	.
-	-	.	.	.	.	.	.	.	.	.	.	.	.

referring to x_2 by a similar table or an abridged version, depending on whether equations (26) or (28) are used. The results of the trapezoid integration are introduced into column (2), differences in columns (3) to (6) are computed, and then column (7) is filled with the help of equations (31), identifying $\dot{y}$ with $\ddot{x}_1$. From the increments in

column (7) values of $\dot{x}_1$ in column (8) may be found which are already better than those of the trapezoid integration. They may at once be used for computing the differences in columns (9) to (12), the increments Δx_1, and the values x_1, again using equations (31).

When this is done with the figures of table 4, it is found that neither the $\dot{x}_1$'s nor the x_1's are capable of improvement, but x_2

is changed appreciably. The final state of the integration for x_2 is shown in table 6. Practically all the correction is due to the first time interval.

TABLE 6

(1)	(2)	(3)	(4)	(5)	(6)	(7)	(8)
t (sec)	$\dot{x}_2$ (in./sec)	$\Delta_1\dot{x}_2$	$\Delta_2\dot{x}_2$	$\Delta_3\dot{x}_2$	$\Delta_4\dot{x}_2$	Δx_2 (in.)	x_2 (in.)
0	119.5						0.988
.0025	105.2	-14.3				0.277	1.265
.0050	100.5	-4.7	9.6			.256	1.521
.0075	97.9	-2.6	2.1	-7.5		.248	1.769
.0100	96.5	-1.4	1.2	-.9	6.6	.242	2.011
.	.	.	.	.	.	.	.
.	.	.	.	.	.	.	.
.	.	.	.	.	.	.	.

When this polynomial method is applied - and the example demonstrates that it may be worth while to do so - then it will be reasonable to use it not only for checking and correcting but also for integrating ahead. To do this, one must extrapolate the polynomial in figure 12 beyond t_n through the next interval and then integrate $\dot{y}$ from t_n to t_{n+1}.

The result may be expressed by the set of differences used before:

$$\Delta y_{n+1} = y_{n+1} - y_n$$

$$= \Delta t \left(\dot{y}_n + \frac{1}{2} \Delta_1 \dot{y}_n + \frac{5}{12} \Delta_2 \dot{y}_n + \frac{3}{8} \Delta_3 \dot{y}_n + \frac{251}{720} \Delta_4 \dot{y}_n \cdots \right) \qquad (32)$$

With the help of this formula one might find in table 5 the values
of $\Delta\dot{x}_1$, $\dot{x}_1$, Δx_1, and x_1 in the next line. But actually it is neces-
sary to use equation (32) only once, preferably for integrating $\ddot{x}_2$
$\left(\text{or } \dot{x}_2, \text{ if } m_2 = 0\right)$, and then approximate values for the other deriva-
tives may be procured in time to do all other integrations at once with
equation (31a) which is more exact and less influenced by the higher
differences.

When thus a new line in all tables (table 1 or 2 and the integra-
tion tables) has been filled, equation (31a) is used repeatedly to
improve x_2 and x_1 as long as they are capable of improvement.

As soon as the columns for the derivatives (columns (2) and (8)
in table 5) fill up, one might extend the difference scheme toward
differences of higher order, but the farther one goes to the right, the
smaller and the more erratic the differences will become and they will
not be able to influence the increments computed from equations (31)
and (32). In general the time step Δt should be chosen such that the
fourth-order difference may be neglected.

Except for the start of the computation which is always a little
irregular, the higher differences should be rather small before they
become erratic; otherwise one must either increase the accuracy of the
derivatives by carrying more digits or decrease the step Δt. If it is
intended to carry more significant figures, one should keep in mind that
a many-digit machine computation is a wasted effort, if somewhere in the
process a figure must be read from a graph, for example, the effective
orifice area A_3 as a function of the stroke x.

In order to check the accuracy of the two methods - trapezoid and
polynomial - an example of a linear shock strut has been computed with
the following data:

$$m_1 = 103.6 \text{ lb sec}^2/\text{in.}$$

$$m_2 = 0$$

$$b = 500 \text{ lb sec/in.}$$

$$k_1 = 2800 \text{ lb/in.}$$

$$k_2 = 12,500 \text{ lb/in.}$$

$$W = 0$$

$$V = 120 \text{ in./sec}$$

The results for this example can be compared with the exact solution, equations (9) and (10). The following values were obtained for the impact force F_1:

t (sec)	F_1 (lb)			
	Exact	$\Delta t = 0.01$ sec		$\Delta t = 0.02$ sec
		Trapezoid	Polynomial	Trapezoid
0.04	38.1×10^3	38.13×10^3	38.03×10^3	38.47×10^3
.08	52.0	52.1	52.0	52.3
.12	56.2	56.2	56.2	56.4
.16	55.7	55.8	55.7	55.8
.20	52.5	52.6	52.6	52.6
.24	47.6		47.6	

Evidently, under these conditions the trapezoid method with $\Delta t = 0.01$ second is good enough. Encouraged by this result, the step Δt has been doubled. The results of the trapezoid integration are shown in the table. The polynomial method proved to be extremely tedious and was not pursued further when after several hours of computation the first four lines had not yet stabilized. However, it was found practical to start with the small interval and double the step as soon as possible. The polynomial method with $\Delta t = 0.01$ second was carried to $t = 0.08$ second, and then the results for $t = 0.02$, 0.04, 0.06, and 0.08 second were used to start the polynomial method with the double interval. This computation was carried up to $t = 0.20$ second and yielded results identical with those obtained for the shorter steps.

Numerical Example

As an illustration of the methods just described an example has been worked out. The data chosen and the metering pin correspond closely to those of a recent American airplane. The data are these:

$$A_1 = A_2 = 39.8 \text{ sq in.}$$

$$\frac{A_o z_o}{A_1} = 23.5 \text{ in.}$$

$$p_o = 310 \text{ lb/sq in.}$$

$$\rho = 8.42 \times 10^{-5} \text{ lb sec}^2/\text{in.}^4$$

$$\gamma = 1.1$$

$$k_2 = 12{,}500 \text{ lb/in.}$$

$$W_1 = 0$$

$$V = 10 \text{ ft/sec}$$

The effective orifice area is shown by the heavy line in figure 13 as a function of the stroke x. The low part at the left-hand side of the diagram represents the bulbous end of the metering pin.

The shock strut is prestressed with the force

$$F_o = p_o A_2 = 12{,}350 \text{ lb}$$

Until the impact force has reached this value, only the tire is deformed and the simple formulas mentioned after equations (26) apply. They yield $t_o = 0.0088$ second, $X_o = 0.988$ inch, and $V_o = 119.5$ inches per second. These are the initial conditions for the numerical integration of equations (25) and (28). This integration was started by the trapezoid method, using equations (29) and (30), and the time step Δt was so chosen that at least a few intervals would pass before the first break in the curve $A_3 = A_3(x)$ was reached. This is possible with $\Delta t = 0.0025$ second, and the first lines of this computation are shown in tables 3 and 4 (where t is counted from the beginning of this integration, not from the first contact between tire and runway). When four steps were completed, the polynomial method was started and the results of these steps were improved. The computation was carried on to $t = 0.0250$ second with $x = 0.571$ inch, $x_1 = 3.907$ inches, and $x_2 = 3.336$ inches. This is sufficiently far past the first break in

$A_3(x)$ that it was possible to double the step. A new integration table was started with the results for $t = 0.010$, 0.015, 0.020, and 0.025 second and it was carried on with $\Delta t = 0.005$ second until $t = 0.060$ second with $x = 1.939$ inches. The next step would have led beyond the second break in the curve $A_3(x)$ and hence to large values in the difference schemes.

Therefore, it was necessary to return to the shorter time step $\Delta t = 0.0025$ second. This makes it necessary to interpolate values for the half intervals. To keep up with the accuracy of the integration, this must be done with the help of the same interpolation parabolas from which equations (31) and (32) are derived. With the notations used the following formula holds:

$$\dot{y}_{n+\frac{1}{2}} = \frac{1}{2}\left(\dot{y}_n + \dot{y}_{n+1}\right) - \frac{1}{16}\left(\Delta_2\dot{y}_{n+1} + \Delta_2\dot{y}_{n+2}\right) + \frac{3}{256}\left(\Delta_4\dot{y}_{n+2} + \Delta_4\dot{y}_{n+3}\right) \quad (33)$$

in which the last term is often negligibly small.

With the help of this formula a new integration table was started, beginning with $t = 0.0450$, 0.0475, . . . second. When it came to $t = 0.0775$ second, the next and last break in the A_3 diagram was reached and the higher differences rose so high that it became necessary to reduce the step to 0.00125 second. Eight lines beyond the discontinuity the step was increased to $\Delta t = 0.0025$ second and soon thereafter to 0.005 second. At $t = 0.14$ second it was realized that the higher differences had become so small that the interval could again be doubled, and with $\Delta t = 0.01$ second the computation was carried until $t = 0.27$ second, when $\dot{x}$ became negative.

The example which was chosen here as a test specimen for the numerical integration is one of the most irregular possible. Most of the computation effort was spent on the bulbous end of the metering pin. As soon as the last corner in figure 13 was passed, the work proceeded rather quickly to its end. When the pin is shaped more gently, or when there is no pin at all, it will be possible to start, say, with $\Delta t = 0.005$ second and to change after some time to $\Delta t = 0.01$ second, without the many tedious changes which were necessary in the present case.

The results of the computation are shown in figures 14 and 15. There is a double time scale in the diagrams, one beginning at the first contact and one at the time t_0 when the numerical integration begins.

Figure 14 shows the stroke x and the displacement x_1 of the airplane. There is a first, short phase during which only the tire is

deformed and $x \equiv 0$. Then the shock strut begins to work but, because
of the bulbous end of the metering pin, the strut collapses, at first
rather slowly. Later it catches up, and the curves x and x_1 approach
each other, indicating that the load maximum is passed and that the tire
expands.

Figure 15 shows the load and its breakdown into the damping force
and the elastic (air) force according to the two terms of equation (25).
Because of the bulbous end of the metering pin the damping force builds
up rapidly, but then the orifice opens up and the increasing air pres-
sure in the shock strut cannot compensate the decline of the damping
force.

Dimensioning of Metering Pin

For reasons of weight saving it is desirable that the shock-strut
force rise quickly to a high value and then remain at this height for a
sufficient time to bring the mass m_1 to rest. As a practical means
for this purpose, the metering pin has been introduced into the design
of shock struts. Now, since there is but one metering pin, it will not
be possible to obtain ideal results for different impact conditions, but
it is possible to pick out one landing case of particular importance and
to shape the metering pin so that in this case a desired load history is
obtained. The shape of the pin which has been found for this case must,
of course, be subjected to a critical study in two respects: It must be
acceptable to the workshop, and it must yield at least tolerable load-
time diagrams under other landing conditions. The final compromise is
a true engineering decision which cannot be replaced by an analytical
device.

There is no need to specify exactly how the impact force should rise
from zero up to a certain level. In this first part of the load history
the tire has an important influence, and it will be enough to choose the
orifice opening A_3 so that not too much stroke is lost while the force
builds up.

But when at a certain time $t = t'$ the force F_1 has reached a
certain value, say $F_1 = F'$, then it may be desirable to keep it constant
on this level. If it is agreed to neglect the unsprung mass m_2 equa-
tions (28) are simply

$$m_1\ddot{x}_1 + F' = W_1 \tag{34a}$$

$$F' = k_2 x_2 \tag{34b}$$

and it follows at once from equation (34b) that $x_2 = $ Constant, say,

$$x_2 = x_2'$$

$$\dot{x}_2 = 0$$

Equation (34a) presents a simple integration problem and yields

$$\dot{x}_1 = \dot{x}_1' + \frac{W_1 - F'}{m_1}(t - t')$$

$$x_1 = x_1' + \dot{x}_1'(t - t') + \frac{W_1 - F'}{2m_1}(t - t')^2$$

where $\dot{x}_1'$ and x_1' are the values which the variables have assumed
at $t = t'$. From equation (28c)

$$\dot{x} = \dot{x}_1$$

$$x = x_1 - x_2'$$

and these values may now be introduced in equation (25) of the oleo strut,
which then yields A_3 :

$$\frac{1}{A_3{}^2} = \frac{2}{\rho A_2{}^3 \dot{x}^2}\left[F' - A_1 p_0\left(\frac{z_o A_o}{z_o A_o - x A_1}\right)^{\gamma}\right] \tag{35}$$

This idea has been applied in two ways to the numerical example of
the preceding section.

When looking at figure 15, one might think it useful to keep F_1
for some time on its peak level, thus decelerating faster the vertical

motion of the airplane without imposing a higher dynamic load on it.
This would result in a saving in stroke and hence in weight of the
shock strut. In this way the curves marked "I" in figures 16 and 17
have been obtained. The corresponding orifice area is shown in fig-
ure 13 by the line I. To keep the impact force at its peak level, the
orifice area must be decreased relative to the original design, and it
comes down to zero when the motion of the airplane is stopped. The
steep descent at the end of this curve is, of course, not acceptable
for the design, since it means a complete plugging of the orifice and
would lead to a high load peak in a case of harder landing; but the
upper part of the curve may lead to an improvement of the design.

One might think of another modification of the load-time curve,
cutting away the peak and keeping F_1 as long as feasible on a medium
level, say at $F' = 46,600$ pounds. When this is done, the curves
marked "II" in figures 13, 16, and 17 result. They show that in this
case a slightly longer stroke is needed than in the original design,
but there is a considerable saving in dynamic load.

Since the rise of F_1 is interrupted in this case, the orifice
must be opened wider, and figure 13 shows that most of the bulbous end
of the pin must be removed. The transition must, of course, be smoother
than that shown in the diagram, and this would lead to a rounding of the
corner in the load-time diagram (fig. 17). Except for this necessary
modification and for the steep end of the A_3 curve, the solution seems
acceptable, provided that the pin shaped in this way proves to be satis-
factory in other landing cases.

But there is still one essential point that needs discussion.
Figure 18 shows the velocities $\dot{x}_1$ and $\dot{x}$ for all three cases. For
the original pin heavier lines have been used and the two modifications
are marked "I" and "II." The first modification does not show anything
in particular, but for the second modified pin $\dot{x}$ jumps suddenly from
one value to another and so does $\dot{x}_2 = \dot{x}_1 - \dot{x}$. Now, a sudden change of
the velocity $\dot{x}_2$ will, of course, meet with the inertia of the unsprung
mass, and the metering pin II cannot be accepted without discussing this
influence.

Starting from equations (26) and putting $F_1 = F'$:

$$m_1\ddot{x}_1 = W_1 - F'$$

$$m_2\ddot{x}_2 + k_2 x_2 = F'$$

The first of these equations is identical with equation (34a), and the second yields an undamped vibration:

$$x_2 = \frac{F'}{k_2} + A \cos \omega(t - t') + B \sin \omega(t - t')$$

$$\omega = \sqrt{k_2/m_2}$$

Now, at $t = t'$, when this vibration begins,

$$x_2 = x_2' = F'/k_2$$

$$\dot{x}_2 = \dot{x}_2'$$

and hence

$$x_2 = x_2' + \frac{\dot{x}_2'}{\omega} \sin \omega(t - t')$$

When it is assumed in the example that $m_2/m_1 = 0.025$, the circular frequency of these vibrations is $\omega = 69.5$ second^{-1}, that is, about 10 cycles per second.

The stroke x will show the same undulation as x_2 and so will the metering pin. Of course, nobody would think of building a metering pin of that shape, in particular since the length and location of these undulations would depend on the arbitrary choice of the conditions under which F_1 is kept constant. As soon as a streamlined metering pin is chosen corresponding to the simplified analysis, the force F_1 will fluctuate slightly and thus provide the necessary damping for the transient vibrations of x_2 and x.

There is still a better way of handling this last question. Since it is not feasible anyway to make a metering pin with a sudden change of cross section, it is better to assume a force diagram on which the corner is well-rounded, say by a parabola

$$F_1 = c_1 + c_2 t + c_3 t^2$$

which is so chosen that there is no large discontinuity in dF_1/dt.

When this force-time relation is introduced into the equations of the landing gear, they may easily be integrated, and the resulting expressions for x and $\dot{x}$ along with F may be introduced into equation (35) to find A_3 and hence the cross section of the metering pin.

The short broken line at the outset of the horizontal line marked "II" in figure 17 represents such a parabolic rounding of a corner in the force diagram. The corresponding values of $\dot{x}$ and A_3 have been indicated by broken lines in figures 18 and 13. One may recognize that no great change of the metering pin is needed to make the wheel motion much smoother, and the corner in the force diagram might still be rounded much more without a substantial loss of deceleration for the airplane.

ADDITIONAL NONLINEARITIES

Tire

The elastic resistance of the tire depends only in small part on the elasticity of the rubber and is essentially due to the compression of the enclosed air. During the landing impact this compression is nearly adiabatic and therefore the relation between the tire pressure and the deflection x_2 is nonlinear. On the other hand, the relation between the pressure and the force F_2 is nonlinear also because the tire flattens. On the whole, these and some other influences seem to compensate to some extent, and load-deflection curves from tests may be fairly well approximated by a straight line. This is illustrated by figure 19 which shows such a test result.

For design purposes it does not seem worth while to replace, under these circumstances, the linear relation (equation (1a)) by anything more complicated. However, for the evaluation of tests it may be advisable to use the best available information on the behavior of the tire.

The nonlinearity of the tire becomes severe when it comes to bottoming. Then the force F_2 may rise to high values without an appreciable further increase of x_2. In general, bottoming should, of course, be avoided, but when it comes into consideration, then equation (1a) can no longer be applied, and it must be replaced by the general relation

$$F_2 = F_2\left(x_2\right)$$

which represents an empirical function determined from tests. The
equations of motion are then these:

$$m_1\ddot{x}_1 + F_1(\dot{x}, x) = W_1 \tag{36a}$$

$$m_2\ddot{x}_2 - F_1(\dot{x}, x) + F_2(x_2) = 0 \tag{36b}$$

instead of equations (26a) and (26b).

Because of the prestressing of the oleo strut these equations are
not valid until the shock-strut force has reached the prestress value F_o.
For this initial phase of the impact the procedure described in the
paragraph following equation (26c) must be applied. Since it covers
but a small part of the whole impact, one may use there the linear
law $F_2 = k_2 x_2$, the spring constant k_2 being taken from the initial
tangent of the load-deflection curve of the tire:

$$k_2 = \left[\frac{dF_2(x_2)}{dx_2}\right]_{x_2=0}$$

For equations (36a) and (36b) then the initial conditions (equa-
tions (27)) are the same as those for equations (26). The equations are
solved by numerical integration and table 1 may be adopted, changing
only the heading of column (9) where F_2 is written instead of $k_2 x_2$
and then using a graph of the function $F_2(x_2)$ to fill this column.

In most cases it will be possible to neglect the mass m_2. Then
equations (36) are rewritten in the form

$$m_1\ddot{x}_1 = W_1 - F_2(x_2) \tag{37a}$$

$$F_1(\dot{x}, x) = F_2(x_2) \tag{37b}$$

which corresponds to equations (28). For the numerical integration use
table 2, writing $F_2 = F_1$ at the top of column (6) and filling this
column with the help of the graph for $F_2(x_2)$.

In both cases, equations (36) and (37), the integration step must be decreased appropriately when approaching the region where the tire bottoms.

Kinematic Nonlinearities

In the equations of motion one needs the second derivatives of the displacements x_1 and x_2, the accelerations of the masses m_1 and m_2, respectively. For the shock strut, the stroke x is needed. Thus far it has always been assumed that x is equal to the difference $x_1 - x_2$. However, this relation holds only in the simple case, when the upper part of the shock strut (usually the barrel) is rigidly connected with the airframe and the wheel is attached directly to the lower part (piston). A correction is already needed when the shock strut is inclined from the vertical (fig. 20). In this case

$$x = \frac{x_1 - x_2}{\cos \alpha}$$

The changes which this relation requires in the intergration schemes are obvious and there is no need to discuss them in detail.

However, there are cases in which the relation between x and $\left(x_1 - x_2\right)$ is nonlinear. Figure 21 illustrates what is meant. Most of these devices have disappeared from current practice, but in a time of rapid development it is advisable to discuss briefly how similar cases may be handled. For all these landing gears a nonlinear relation

$$x = f\left(x_1 - x_2\right) \tag{38}$$

can be established by trigonometric methods. By differentiating it with respect to time, the relation

$$\dot{x} = \frac{df\left(x_1 - x_2\right)}{d\left(x_1 - x_2\right)}\left(\dot{x}_1 - \dot{x}_2\right)$$

$$= f'\left(x_1 - x_2\right)\left(\dot{x}_1 - \dot{x}_2\right) \tag{39}$$

is derived. The above two equations take the place of equation (26c) and the corresponding relation for the velocities.

Table 1 must now be replaced by table 7, in which columns (5a), (6a), and (6b) have been added. Columns (5a) and (6b) are filled from the preceding ones and column (6a) is filled from a formula or a graph

TABLE 7

(1)	(2)	(3)	(4)	(5)	(5a)	(6)	(6a)	(6b)	(7)	(8)	(9)	(10)	(11)	(12)
t	x_1	$\dot{x}_1$	x_2	$\dot{x}_2$	$x_1 - x_2$	x	f'	$\dot{x}_1 - \dot{x}_2$	$\dot{x}$	F_1	$k_2 x_2$	$\ddot{x}_2$	$W_1 - F_1$	$\ddot{x}_1$

for $f'(x_1 - x_2)$. Then equations (38) and (39) are used to fill columns (6) and (7). Everything else is done as explained for table 1.

When m_2 is neglected, table 8 is used instead of table 2. Again additional columns for $(x_1 - x_2)$, $(\dot{x}_1 - \dot{x}_2)$, and f' are provided. Column (5) is filled with the help of equation (38); column (7a), from

TABLE 8

(1)	(2)	(3)	(4)	(4a)	(5)	(6)	(7)	(7a)	(7b)	(8)	(9)	(10)
t	x_1	$\dot{x}_1$	x_2	$x_1 - x_2$	x	F_1	$\dot{x}$	f'	$\dot{x}_1 - \dot{x}_2$	$\ddot{x}_2$	$W_1 - F_1$	$\ddot{x}_1$

column (4a) with a graph or formula for $f'(x_1 - x_2)$; and column (7b), with equation (39).

These are very simple changes, the numerical integration being a very flexible instrument that can be adapted to almost every special requirement.

THE AIRPLANE AS A WHOLE

Introduction

In most investigations of landing gears the airplane is represented by a single mass m_1 riding on a system of springs and dampers, with perhaps a small additional mass m_2 representing the wheel. All the preceding sections of this report are exclusively concerned with this model.

However, the real airplane is a three-dimensional structure, and when one or more of its wheels hit the ground, it may receive not only a vertical acceleration but also angular accelerations about different axes. These angular accelerations and the rotatory motion resulting from them will, of course, influence the landing impact.

A detailed study of this phenomenon leads into rather lengthy computations. Their quantitative results will depend on many details and may vary widely between different types of airplanes. This section will therefore be restricted to some general considerations concerning the best method of analysis.

There are two principal problems, the symmetric case in which both wheels of the main landing gear strike the ground simultaneously and in identical conditions, either earlier or later than the auxiliary gear, and the asymmetric case in which the two wheels of the main gear touch the ground one after the other.

Symmetric Impact

Figure 22 shows the side view of an airplane as far as it is of interest for the present purposes. The point C is the center of gravity where the mass m is located. To the right is the main gear; to the left, the auxiliary gear which may be either a nose gear or a tail gear.

In figure 22 the airplane is shown in the position which it has at the time $t = 0$, when the main gear makes its first contact with the runway. From this time an impact force F_1 of increasing magnitude will act in each main gear and it will cause both a deceleration of the vertical movement of the center of gravity and a pitching motion about this point. The equations of motion are

$$m\ddot{z} = -2F_1 + W$$

$$I_y\dot{\omega} = -2F_1 a$$

(40)

where I_y is the moment of inertia of the airplane with respect to its transverse axis.

The resultant acceleration at the upper end of the main landing gear will be

$$\ddot{x}_1 = \ddot{z} + a\dot{\omega}$$

$$= -\frac{2F_1}{m} - \frac{2F_1 a^2}{I_y} + \frac{W}{m}$$

$$= -\frac{2F_1}{m}\left(1 + \frac{ma^2}{I_y}\right) + \frac{W}{m}$$

In the section "Linear Spring-Damper Systems" there was written

$$\ddot{x}_1 = -\frac{F_1}{m_1} + \frac{W_1}{m_1}$$

and the two expressions are equivalent if one chooses

$$m_1 = \frac{m}{2\left(1 + \frac{ma^2}{I_y}\right)}$$

$$= \frac{m}{2}\frac{i_y^2}{a^2 + i_y^2}$$

$$W_1 = \frac{W}{2} \frac{i_y^2}{a^2 + i_y^2}$$

where $i_y = \sqrt{I_y/m}$ is the radius of gyration. These formulas show that it is perfectly justifiable to study an isolated landing gear, provided one does not simply use as mass m_1 one-half of the airplane mass. However, this procedure is subject to two essential limitations: It can be applied only until the auxiliary gear comes into action and must at least be modified when the rotation of the airplane leads to a substantial change of the angle of incidence of the wing and hence to a change of the load W.

Consider the second point first. The angular position of the airplane is determined by the angle α between the ground and a reference line in the plane of symmetry of the airplane. This reference line is so chosen that $\alpha = 0$ when all three wheels of the airplane just touch the ground without pressure. The angle α which is so defined is not identical with the angle of incidence of the wings, but the two differ only by a constant which depends on the design of the airplane.

Since only small values of α need be considered, it may be assumed that the lift and hence W is a linear function of α, say:

$$W = W' + W''\alpha$$

but since one must use numerical integration methods anyway an arbitrary function

$$W = W(\alpha)$$

may be assumed when this appears to be necessary. The part of this weight which must be attributed to one main landing gear is then

$$W_1(\alpha) = W(\alpha)\frac{i_y^2}{2\left(a^2 + i_y^2\right)} \tag{41}$$

Equations of motion (40) are now written in the following form:

$$\ddot{x}_1 = -\frac{1}{m_1}\left(2F_1 - W_1\right) \tag{42a}$$

$$\ddot{\alpha} = -\frac{2a}{I_y} F_1 \tag{42b}$$

Additionally, there is a relation which connects F_1 with x and $\dot{x}$, for example, equation (25) of the oleo strut, the relation $x = x_1 - x_2$, and the elastic equation of the tire $F_2 = F_1 = k_2 x_2$. Table 2 which is used for the one-gear problem must now be extended so that it may take care of equation (42b). It looks then as shown in table 9:

TABLE 9

(1)	(2)	(3)	(4)	(5)	(6)	(7)	(8)	(9)	(10)	(11)	(12)	(13)	(14)
t	x_1	$\dot{x}_1$	x_2	x	α	$\dot{\alpha}$	F_1	$\dot{x}$	$\dot{x}_2$	W_1	$W_1 - F_1$	$\ddot{x}_1$	$\ddot{\alpha}$
0													

Columns (2) to (5) and (8) to (10) are treated exactly as are the corresponding columns of table 2; the first line in columns (6) and (7) is filled in from two additional boundary conditions (α given, $\dot{\alpha} = 0$). Also the starting value of W_1 will be known and must, of course, check with column (6) and equation (41). Column (12) is self-explanatory, and columns (13) and (14) follow from equations (42). Besides the tables for the integration of $\ddot{x}_1$, $\dot{x}_1$, and $\dot{x}_2$, an additional table is now needed to integrate $\ddot{\alpha}$ and $\dot{\alpha}$. With the results of these integrations the second line may be started.

Of course, this analysis does not consider the possibility that the pilot uses the controls to counteract the pitching movement of the airplane. If he does so, a human element comes into play which is not easily incorporated in mathematical formulas. This uncertainty may upset the usefulness of the procedure and will justify the application

of the simpler table given previously. This simplification, commonly
used in landing-gear analysis, is still more justified by the results
represented in figure 6, which show that the exact magnitude of the
effective weight W_1 is of secondary importance for the interesting
portion of the impact.

Whether a simple one-gear analysis is made or the variability of
W_1 is taken into account, this computation ends at the moment when the
auxiliary gear comes into action. The time $t = t'$ when this occurs
is found in the following way: During the first phase of motion the
acceleration at the upper end of the auxiliary gear is:

$$\ddot{x}_3 = \ddot{z} - b\dot{\omega}$$

$$= -\frac{2F_1}{m}\left(1 - \frac{ab}{i_y^2}\right) + \frac{W}{m}$$

When it is assumed that the airplane approaches the ground with the
vertical velocity V, but without an angular velocity, then the velocity
$\dot{x}_3$ for $t > 0$ is

$$\dot{x}_3 = V - \frac{2}{m}\frac{i_y^2 - ab}{i_y^2}\int_0^t F_1\, dt + \frac{1}{m}\int_0^t W\, dt \qquad (43)$$

Under the integral signs F_1 and W must be introduced as functions
of t according to the analysis of the main gear.

The displacement x_3 of the auxiliary gear is best counted from
the position in which the wheel just touches the ground. When the
airplane lands at an angle α (fig. 22), then $x_3 = -(a + b)\alpha$ at
$t = 0$. For $t > 0$

$$x_3 = -(a + b)\alpha + \int_0^t \dot{x}_3\, dt \qquad (44)$$

and the time when this equation yields $x_3 = 0$ is the time $t = t'$.

When $W = 0$ and $ab < i_y^2$, the velocity $\dot{x}_3$ will decrease and the impact of the auxiliary gear will be softer than it would be if this gear had hit the ground before the main gear. If $W \neq 0$, there is an additional positive term in equation (43) and, since the airplane is still falling under the influence of the force W, the velocity $\dot{x}_3$ may increase. When $ab > i_y^2$, then $\dot{x}_3$ will certainly increase, possibly even very much so, and the auxiliary gear may strike the runway rather forcibly.

When all wheels are in contact with the ground, the equations of motion are rather involved. When all landing gears have a spring-damper unit as a shock strut, no damping in the tire, and no unsprung mass, the problem is of sixth order. It is of little value to establish the formulas for the linear case, but it is useful to develop a numerical procedure which may be applied in linear as well as in nonlinear cases.

The equations of motion contain now the forces in main and auxiliary gears (fig. 23):

$$\left.\begin{aligned} m\ddot{z} &= -2F_1 - F_3 + W \\[2em] I_y\dot{\omega} &= -2F_1 a + F_3 b \end{aligned}\right\} \tag{45}$$

Then there are two kinematic relations

$$\left.\begin{aligned} \dot{x}_1 &= \dot{z} + a\omega \\[1em] \dot{x}_3 &= \dot{z} - b\omega \end{aligned}\right\} \tag{46}$$

Differentiating there and then introducing $\ddot{z}$ and $\dot{\omega}$ from equations (45) yield

$$\left.\begin{aligned} \ddot{x}_1 &= -\frac{2F_1}{m}\left(1 + \frac{a^2}{i_y^2}\right) - \frac{F_3}{m}\left(1 - \frac{ab}{i_y^2}\right) + \frac{W}{m} \\[2em] \ddot{x}_3 &= -\frac{2F_1}{m}\left(1 - \frac{ab}{i_y^2}\right) - \frac{F_3}{m}\left(1 + \frac{b^2}{i_y^2}\right) + \frac{W}{m} \end{aligned}\right\} \tag{47}$$

These equations may be used in the following way: For each landing
gear a single-gear analysis is started according to the instructions
given in the section "Intentional Nonlinearities." For the main gear
it begins at $t = 0$ and runs exactly as explained there until $t = t'$.
For the auxiliary gear it begins at $t = t'$ with $x_3 = 0$ and the
value of $\dot{x}_3$ which follows from equation (43). When it is not desired
to neglect the unsprung mass, table 1 is used, otherwise table 2. In
either case the line for $t = t'$ may be filled up to the last two
columns, but the last two columns are replaced by some columns which are
adapted to equations (47). They yield $\ddot{x}_1$ and $\ddot{x}_3$ in terms of the
forces F of both tables, and these values are now integrated just as
was done with $\ddot{x}_1$ in table 4.

A step-by-step integration of this kind requires twice as much
time as a single-gear analysis and will yield everything needed for
both gears.

One-Wheel Landing

It is possible that a landing airplane may approach the runway
with one wing low and that the wheels of the main gear do not hit the
runway at the same time (fig. 24). There are then again two phases, a
first one while only one wheel is in contact with the ground and a
second one when both wheels are.

In the first phase there is only one force F_1, having the
distances a and c from the lateral and longitudinal axes, respec-
tively. It produces the following accelerations:

Vertical at center of gravity:

$$m\ddot{z} = -F_1 + W$$

Angular with respect to lateral axis:

$$I_y \dot{\omega}_y = -F_1 a$$

Angular with respect to longitudinal axis:

$$I_x \dot{\omega}_x = -F_1 c$$

The resulting acceleration at the upper end of the active landing gear is

$$\ddot{x}_1 = \ddot{z} + a\dot{\omega}_y + c\dot{\omega}_x$$

and when use is made of the preceding equations there is obtained

$$\ddot{x}_1 = -\frac{F_1}{m}\left(1 + \frac{ma^2}{I_y} + \frac{mc^2}{I_x}\right) + \frac{W}{m}$$

Again it is useful to introduce the radii of gyration by:

$$i_x{}^2 = I_x/m$$

$$i_y{}^2 = I_y/m$$

and to write

$$\ddot{x}_1 = -\frac{F_1}{m}\left(1 + \frac{a^2}{i_y{}^2} + \frac{c^2}{i_x{}^2}\right) + \frac{W}{m}$$

When this is compared with the relation

$$\ddot{x}_1 = -\frac{F_1}{m_1} + \frac{W_1}{m_1}$$

used previously, it is seen that one must put

$$m_1 = \frac{m}{1 + \dfrac{a^2}{i_y{}^2} + \dfrac{c^2}{i_x{}^2}}$$

$$W_1 = W\,\frac{m_1}{m}$$

With these notations the impact problem is again reduced to a one-gear problem until the other wheel meets the ground. The time $t = t''$ at which this will occur may be found in the same way as in the case of a two-point landing.

The acceleration at the top of the second main gear is

$$\ddot{x}_3 = \ddot{z} + a\dot{\omega}_y - c\dot{\omega}_x$$

$$= -\frac{F_1}{m}\left(1 + \frac{a^2}{i_y^2} - \frac{c^2}{i_x^2}\right) + \frac{W}{m}$$

Integrating once yields the velocity:

$$\dot{x}_3 = V - \frac{1}{m}\left(1 + \frac{a^2}{i_y^2} - \frac{c^2}{i_x^2}\right)\int_0^t F_1 \, dt + \frac{W}{m} t$$

and integrating again,

$$x_3 = -2c\beta + \int_0^t \dot{x}_3 \, dt$$

At the time $t = t''$ when $x_3 = 0$, the one-gear problem ends and from then on both main gears must be dealt with simultaneously.

This is done as in the preceding section, but the formulas differ in details because there is still one degree of freedom left, the rotation about the transverse axis of the airplane. During this phase of the landing impact the equations of motion (fig. 25) are as follows:

$$m\ddot{z} = -F_1 - F_3 + W$$

$$I_y\dot{\omega}_y = -\left(F_1 + F_3\right)a$$

$$I_x\dot{\omega}_x = \left(-F_1 + F_3\right)c$$

Besides there are the kinematic relations

$$\ddot{x}_1 = \ddot{z} + a\dot{\omega}_y + c\dot{\omega}_x$$

$$\ddot{x}_3 = \ddot{z} + a\dot{\omega}_y - c\dot{\omega}_x$$

and by combining both sets of equations the following equations are obtained which correspond to equations (47):

$$\left.\begin{array}{l} \ddot{x}_1 = -\dfrac{F_1}{m}\left(1 + \dfrac{a^2}{i_y{}^2} + \dfrac{c^2}{i_x{}^2}\right) - \dfrac{F_3}{m}\left(1 + \dfrac{a^2}{i_y{}^2} - \dfrac{c^2}{i_x{}^2}\right) + \dfrac{W}{m} \\[4mm] \ddot{x}_3 = -\dfrac{F_1}{m}\left(1 + \dfrac{a^2}{i_y{}^2} - \dfrac{c^2}{i_x{}^2}\right) - \dfrac{F_3}{m}\left(1 + \dfrac{a^2}{i_y{}^2} + \dfrac{c^2}{i_x{}^2}\right) + \dfrac{W}{m} \end{array}\right\} \quad (48)$$

These equations may be handled exactly in the same way as equations (47), with, however, the restriction that the auxiliary gear must still be off the ground. As soon as it makes contact, the relations become more involved, but it seems at present not necessary to elaborate the details of the third phase of the impact which then will follow.

REVIEW OF GERMAN LITERATURE ON LANDING-GEAR IMPACT

Before the last war in Germany almost no theoretical work was done on landing-gear problems, and it seems also that in other countries interest was low.

During the war in Germany new and unexpected demands could frequently best be met by adapting an existing airplane type, with its well-established mass-production facilities. Such modifications usually resulted in an increase of weight without supplying additional space into which a larger wheel could be retracted. Frequent tire troubles were the unavoidable consequence, resulting in a strong impetus to landing-gear research. All but one of the papers reviewed here belong to this period of wartime research.

When studying this German wartime literature, one must keep in mind during what period and under what circumstances the work was done.

All of these papers appeared in 1943 and 1944 and were thus the outcome
of a rather short period of research. They represent an intensive
attempt to tackle a long-neglected problem. But before the work had
yielded results of final validity, it was cut off early in 1945 by
the national catastrophe. More than 6 years have elapsed and the
landing-load problem has undergone changes. Some of the statements
made in those papers have lost interest, others are no longer applicable
without modification, and most of the analytical methods are either
oversimplified or too complicated.

Nevertheless, it is still worth while to survey this literature
briefly because it contains many of the ideas and methods which are
still the basis of landing-gear analysis. Indeed, in writing this
report the author has drawn much useful information from the German
publications which are reviewed on the following pages.

The goal of the early landing-gear research was influenced by the
attitude of official regulations. They required that a drop test be
made in which the upper end of the shock strut was connected with a
mass $\left(m_1\right.$ in the notation of this paper$\left.\right)$ and the two dropped on an
anvil. At the instant when the anvil was struck, the weight W_1 was
compensated by admitting compressed air to two cylinders. The load-
stroke curve obtained by this test was then considered as "the" load-
stroke curve of the shock strut and was employed in all landing cases
which had to be considered in the design of the airplane. Consequently,
the effort of the early research was directed toward the investigation
of load-stroke diagrams of shock struts.

The first paper that must be mentioned here, and the only one that
appeared before the war, was written by Michael (reference 1). It gives
a detailed analysis of the linear spring-damper system but pays only
slight attention to the tire. A special feature of this paper is the
use of spring diagrams in which the force is plotted either against the
stroke with the rate of stroke as a parameter or, inversely, against
the rate of stroke with the stroke as parameter. These diagrams are
shown also for shock struts with dry friction or with velocity-square
dampers, and they are used for a graphical solution of the differential
equation. Such diagrams are no longer possible when a second spring
(the tire) is present, and therefore they have not been employed again
in later papers.

The first papers of the war period were still focused on the load-
stroke diagram. Schlaefke (reference 2) criticized the drop-test method
and suggested replacing the buffered drop test by an unbuffered test,
that is, omitting the air cylinders and with them a possible source of
inaccuracy. His paper uses the theory of the linear spring-damper system
to establish some relations between the results of both tests.

In a later paper (reference 3) the same author realizes that the damping in the oleo strut is far from proportional to the rate of stroke. He compares load-stroke curves for linear and for velocity-square damping and arrives at the strange conclusion that the former look more realistic. The method used for the analysis of the nonlinear problem is of interest. A balance of kinetic and potential energy is established and from it, a differential equation between $\dot{x}$ as dependent and x as independent variable. When it is solved, the damping force (proportional to $\dot{x}^2$) is also known in terms of x. However, this approach is not possible in the presence of a tire.

In the next group of papers the tire makes its appearance. A paper by Kochanowsky (reference 4) gives a very detailed analysis of the oleo-tire combination as shown in figure 1. Kochanowsky finds that the unsprung mass is of no great importance for the landing impact and that the problem may readily be simplified by assuming $m_2 = 0$. The study of this paper (and of many others) is rendered difficult by the author's habit of using for all and everything dimensionless quantities so that the reader has to learn first a system of not very suggestive notations before he can follow the analysis or read the diagrams.

Another paper by Schlaefke (reference 5) covers approximately the same ground.

After having studied the linear oleo-tire system, the next logical step would have been to consider a nonlinear shock strut, but, incidentally, the few papers which did this were older than Kochanowsky's comprehensive paper on the linear system. One of them is by the same author (reference 6), and it was not thought to be a study of a nonlinear case. It is concerned with a special type of spring which has long been used in railroad-car bumpers and was introduced in landing gears. It consists of a pile of rings with conical sides (fig. 26). When it is subjected to an axial compression, the hoop stresses in the rings are alternatively tensile and compressive. During the elastic deformation, the rings slip on one another and the pile becomes shorter. Because of the slip, there is considerable dry friction, and when the load F is decreased, the deformation x is not immediately decreased but follows a law which is described by figure 27. The area of the triangular loop represents a loss of energy and the ring pile may thus be used as a damped spring. Kochanowsky's paper considers a shock-strut and tire combination in which the strut has no other elastic or damping element except such a ring-pile spring. During the first upstroke the analysis is extremely simple, since not even damping appears explicitly in the equations; but when the motion is followed beyond the force maximum, it is linear only in sections but nonlinear on the whole. The paper is an interesting study, but the ring-pile shock strut is not versatile enough to stand the competition with the modern oleo strut, and the problem is now obsolete.

The other paper which considers a nonlinear shock strut is a very
serious and very detailed study by Marquard and Meyer zur Capellen
(reference 7). The authors consider velocity-square damping and
polytropic compression of the air, formulate differential equations,
and integrate them numerically. Unfortunately, the authors overestimate
the accuracy requirements of the analysis. In their tables values are
given to six and even seven significant digits, and consequently they
employ an exact but very tedious method of step-by-step integration.

In addition to the detailed treatment of the nonlinear shock strut,
the paper is remarkable for another reason. It not only considers an
oleo-tire system with a very realistic shock strut, but it also considers
the motion of the whole airplane in its plane of symmetry. In a second
paper (reference 8) the same authors extend their investigation to cases
of unsymmetric landing. But here also the attempt at exactness goes too
far when the decrease of horizontal speed during the short impact time
is taken into consideration. This is pointed out in a paper by Schmitz
(reference 9). This author also considers the pitching motion of the
airplane and includes the ensuing change of the lift, but he falls back
to the old idea of "the" load-stroke curve and fails to realize that
the cooperation between the elastic reaction of the air and the damping
force caused by the orifice depends largely on the conditions of the
impact.

Besides the landing impact, the taxying of the airplane has always
met with interest. Michael's paper (reference 1) pays attention to it,
and Kochanowsky's papers (references 4 and 6) both consider the taxying
impact in full detail. In these papers the statement is made and proved
that when the airplane rolls over a sinusoidal ground swell, the mass m_1
travels practically on a level path and that therefore the analysis may
be made on the assumption that $m_1 = \infty$.

Besides these papers there are two by Schlaefke in which taxying
is considered. One of them (reference 10) covers the same ground as
the corresponding part of Kochanowsky's paper (reference 4). The second
(reference 11) is a short note concerning the impact during the take-off
run. It seems to be the only paper devoted to this subject, and not
much information is found in it.

Additionally, there are a number of reports on experiments. Most
of them were tests made by the airplane manufacturers and served
essentially the purpose of improving a new airplane model to the point
where it was ready for production. Today, it is difficult, if not
impossible, to draw other than qualitative information from these reports
since the airplanes, shock struts, and tires used in these tests no
longer exist and details needed for an analysis may no longer be obtained
readily.

However, one of the experimental papers must be mentioned in this review, a short report of Höke (reference 12) on the experiments he made in the Deutsche Versuchsanstalt für Luftfahrt. He measured, as functions of time, the vertical velocity of the airplane immediately before and during the landing impact and the vertical and lateral forces on the wheel. The fine experimental technique of the velocity measurement is described in the paper.

Stanford University
    Stanford, Calif., November 15, 1951

BIBLIOGRAPHY OF GERMAN LITERATURE

1. Michael, Franz: Theoretische und experimentelle Grundlagen für die
     Untersuchung und Entwicklung von Flugzeugfederungen (Theoretical
     and Experimental Principles of Landing Gear Research and
     Development). Luftfahrtforschung, Bd. 14, Lfg. 8, Aug. 20, 1937,
     pp. 387-416.

2. Schlaefke, K.: Zum Vergleich von gepufferten und ungepufferten
     Federstössen an Flugzeugfahrwerken ("Buffered" and "Unbuffered"
     Impact on Landing Gears). T. B., Bd. 10, Nr. 5, 1943, pp. 129-133.

3. Schlaefke, K.: Zur Kenntnis der Kraftwegdiagramme von
     Flugzeugfederbeinen (On Force-Deflection Diagrams of Shock Struts).

     1. Teilbericht - Vergleich von Diagrammen mit linearer und
          quadratischen Dämpfung (Comparison of Diagrams with Linear
          and Quadratic Damping). T. B., Bd. 11, Nr. 2, 1944, pp. 51-53.

     2. Teilbericht - Näherungsverfahren zum Berechnen der
          Kraftwegdiagramme mit nichtlinearer Federkennlinie und linearer
          oder quadratischer Dämpfung (Approximate Method for the
          Calculation of Force-Deflection Diagrams with a Nonlinear
          Spring Chart and Linear or Quadratic Damping). T. B., Bd. 11,
          Nr. 4, 1944, pp. 105-109.

     3. Teilbericht - Der Landestoss von Ölluftfederbeinen (The Landing
          Impact of Oleo Legs). T. B., Bd. 11, Nr. 5, 1944, pp. 137-141.

4. Kochanowsky, W.: Landestoss und Rollstoss von Fahrwerken mit
     flüssigkeitsgedämpften Schraubenfederbeinen (Landing and Taxying
     Impacts on Oleo Shock Struts). Untersuchungen und Mitteilungen
     Nr. 1423, Deutsche Luftfahrtforschung, Nov. 14, 1944.

5. Schlaefke, K.: Zur Kenntnis der Wechselwirkungen zwischen Federbein
     und Reifen beim Landestoss von Flugzeugfahrwerken (On Reciprocal
     Effects between Shock Strut and Tire in Landing Impact of Airplane
     Undercarriages). T. B., Bd. 10, Nr. 11, 1943, pp. 363-367.

6. Kochanowsky, W.: Landestoss und Rollstoss von Fahrwerken mit
     Ringfederbeinen (Landing and Taxying Impacts on Landing Gears
     with Ring Spring Struts). Forschungsbericht Nr. 1757, Deutsche
     Luftfahrtforschung, Feb. 8, 1943.

7. Marquard, E., and Meyer zur Capellen, W.: Näherungsweise Berechnung der zwischen Fahrgestell und Rumpf beim Landen auftretenden Federungskräfte. Symmetrische Landung (Approximate Calculation of the Forces between Landing Gear and Fuselage of a Landing Aircraft. Symmetric Landing). Forschungsbericht Nr. 1737/1, Tech. H. S. Aachen, 1943.

8. Marquard, E., and Meyer zur Capellen, W.: Näherungsweise Berechnung der zwischen Fahrgestell und Rumpf beim Landen auftretenden Federungskräfte. Unsymmetrische Landung (Approximate Calculation of the Forces between Landing Gear and Fuselage of a Landing Aircraft. Asymmetric Landing). Forschungsbericht Nr. 1737/2, Tech. H. S. Aachen, 1943.

9. Schmitz, G.: Bewegungsvorgang, Stosskräfte und Federwege bei der Landung eines Bugradflugzeuges (Motion, Impact Forces and Spring Strokes in the Landing of a Nose-Wheel Airplane). T. B., Bd. 10, Nr. 12, 1943, pp. 389-392.

10. Schlaefke, K.: Zur Frage der Rollstossbeanspruchung von Flugzeugfahrwerken (On Rolling-Impact Load on Airplane Landing Gears). T. B., Bd. 11, Nr. 9, 1944, pp. 289-295.

11. Schlaefke, K.: Zur Ermittlung der Beanspruchung von Flugzeugfahrwerken beim Start (On the Forces in Landing Gears during Take-Off). T. B., Bd. 10, Nr. 1, 1943, pp. 29-30.

12. Höke, H.: Beanspruchungsmessungen an Fahrwerken bei der Landung und beim Rollen (Measurements of Landing-Gear Loads during Landing and Taxying). Bericht 169, L.G.L., 1943, pp. 28-37.
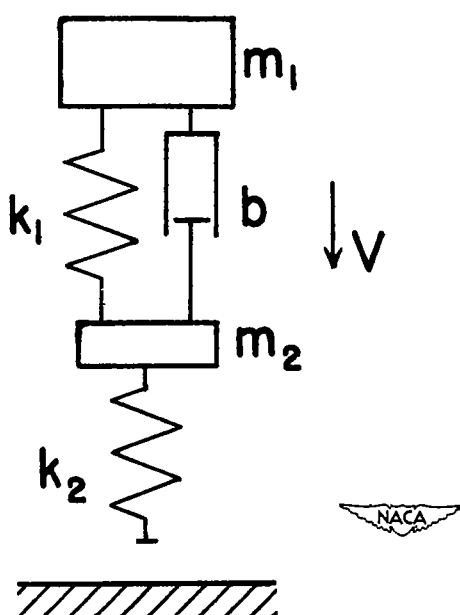
Figure 1.- Representation of shock strut by spring and damper arranged
in parallel.
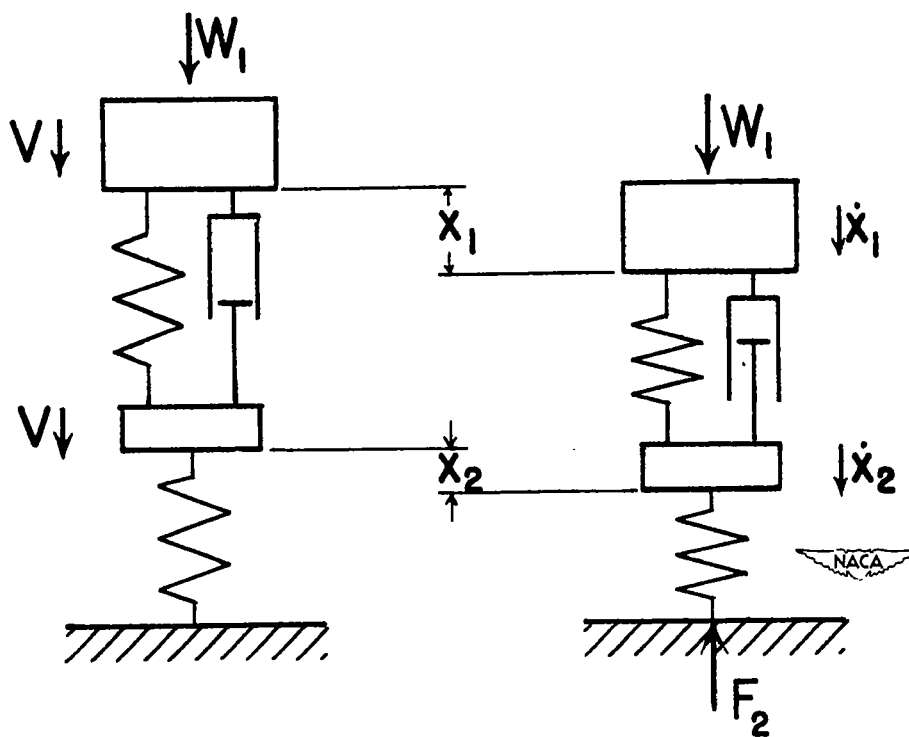
(a) At t = 0.   (b) At some later time.

Figure 2.- Mechanical system in two positions.

F_1/m_1g

$.0\ 5$

0 m_2/m_1

t/T
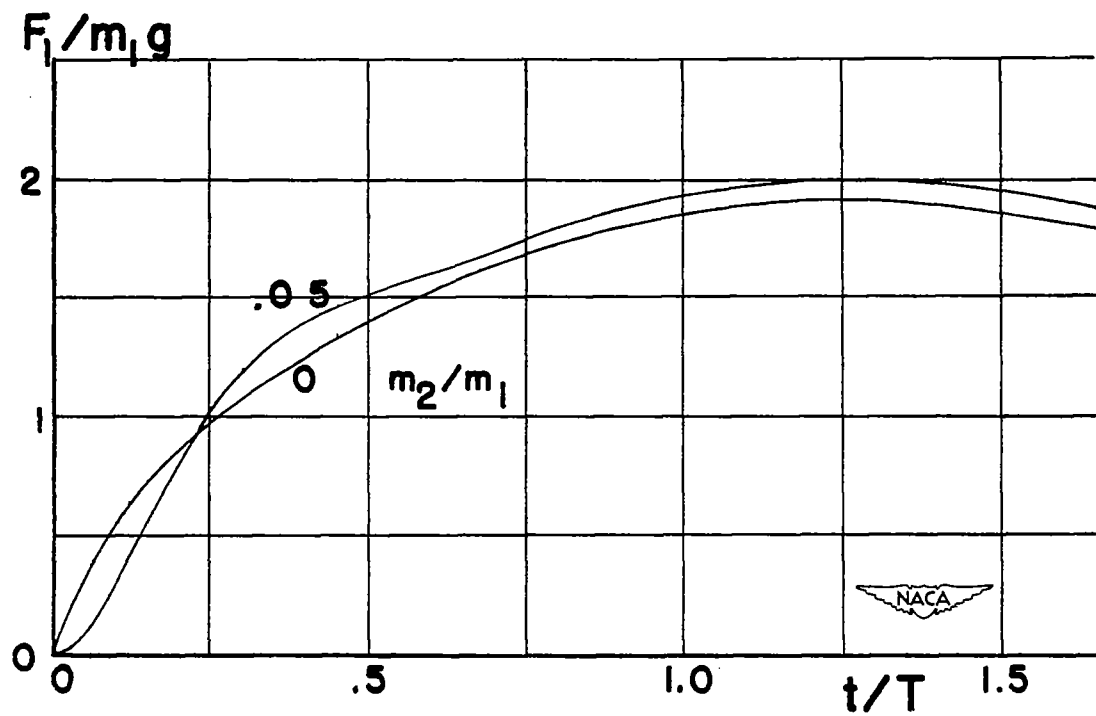
(a) On shock-strut force.

F_2/m_1g

$.0\ 5$

0 m_2/m_1

t/T
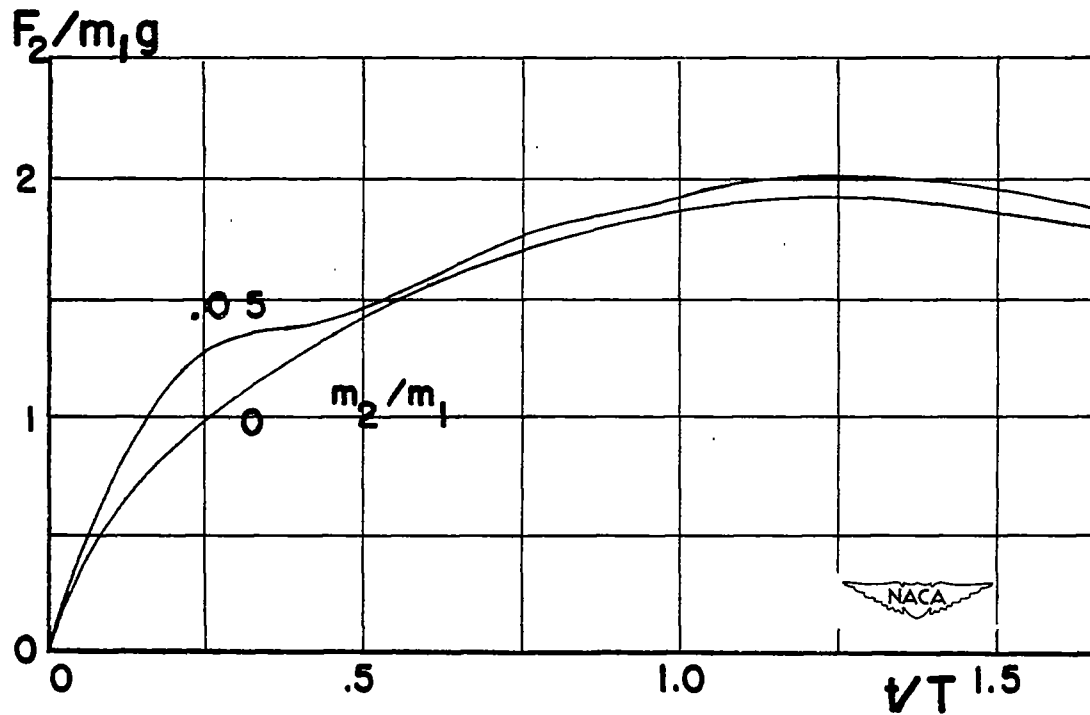
(b) On impact force.

Figure 3.- Influence of unsprung mass.

F_2/m_1g

(a) Force on wheel.

x/δ
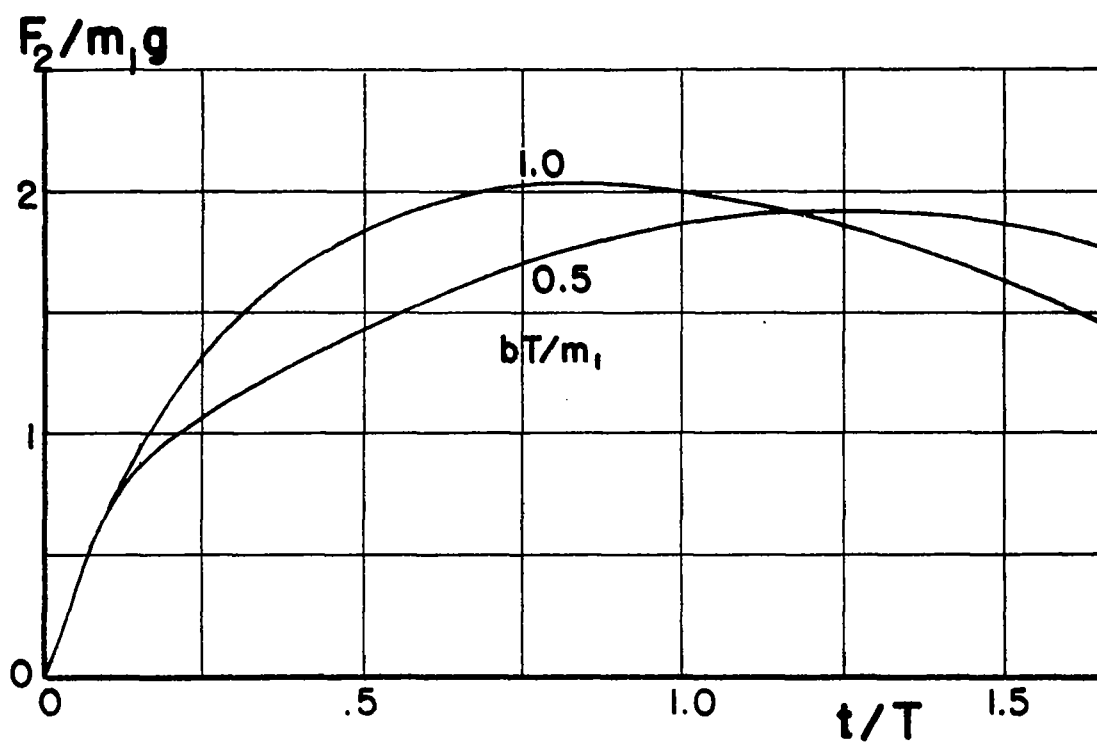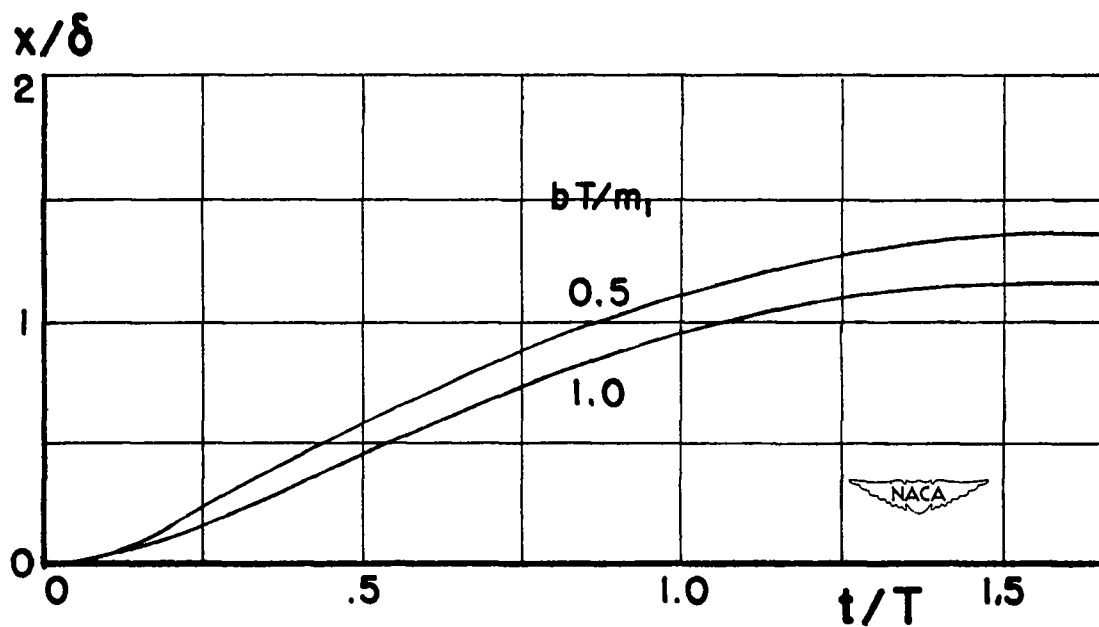
(b) Development of stroke.

Figure 4.- Influence of damping on landing impact.

F_1/m_1g

0.25

0.15

$k_1/(k_1+k_2)$

.5   1.0   t/T   1.5

(a) Force on shock strut.

F_2/m_1g

0.25

0.15

$k_1/(k_1+k_2)$

.5   1.0   t/T   1.5
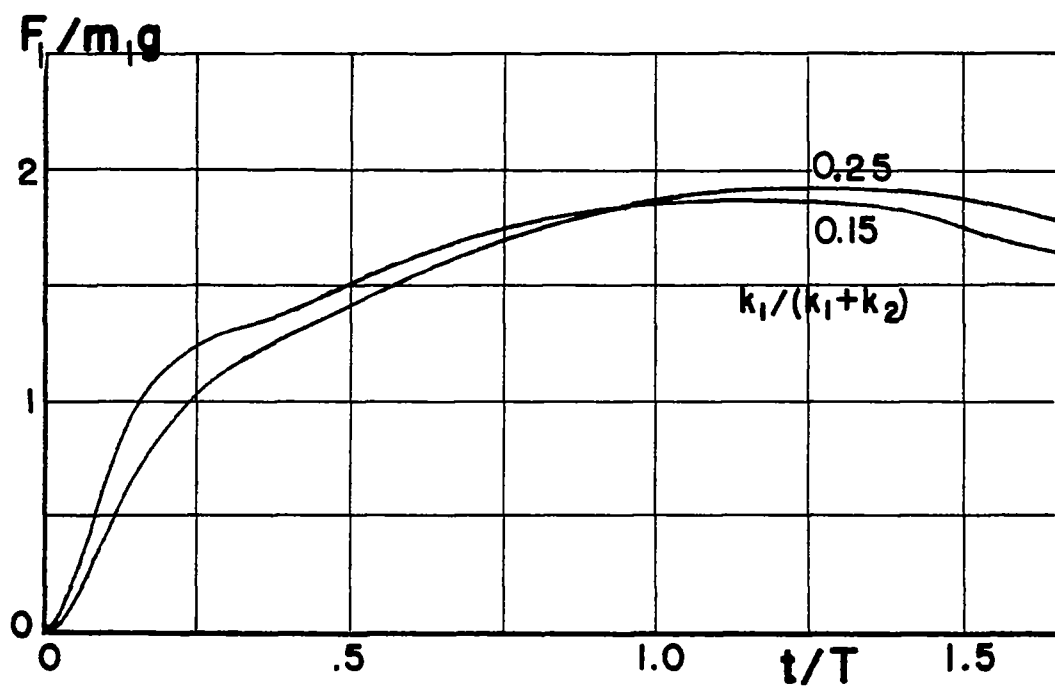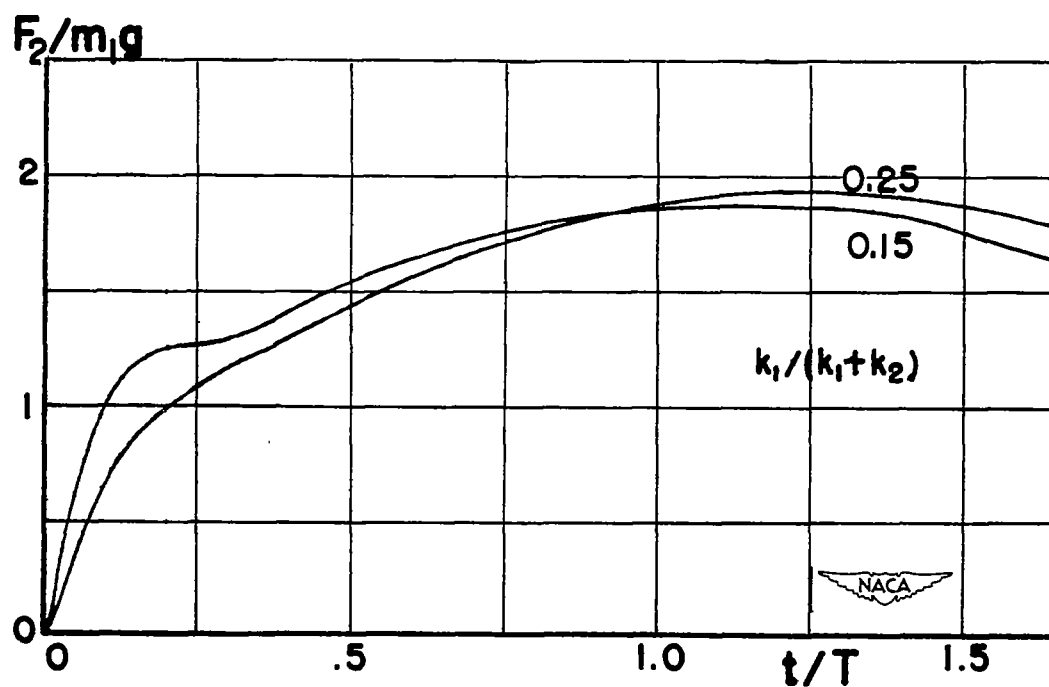
(b) Force on wheel.

Figure 5.- Influence of spring constants on landing impact.
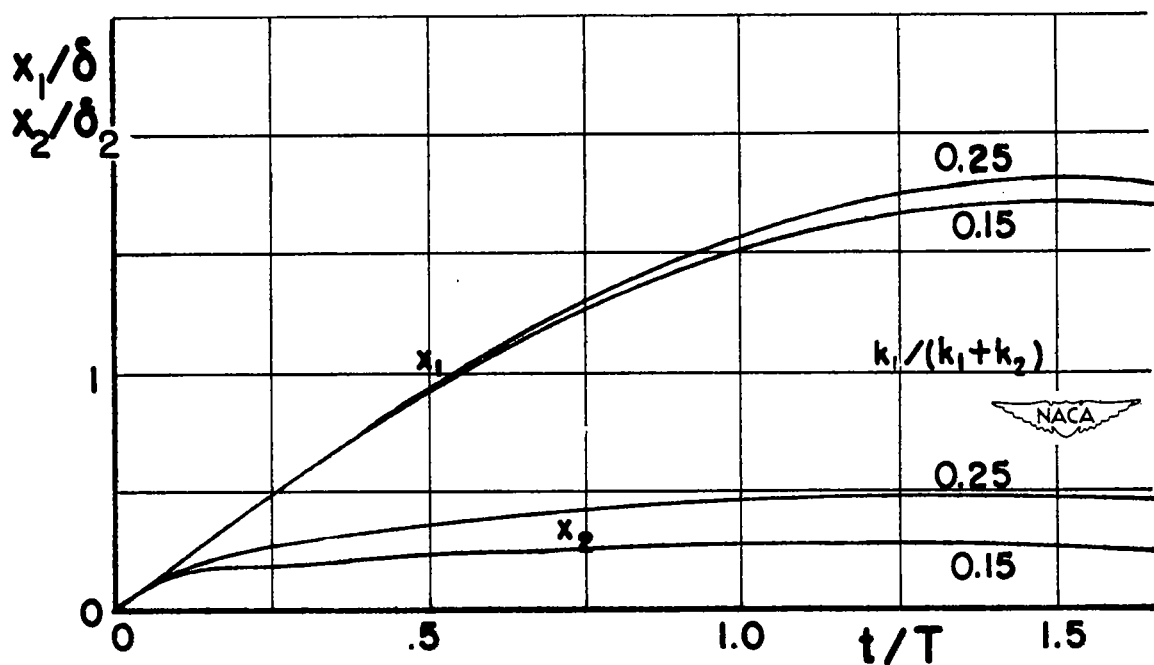
(c) Displacement of airplane and deformation of tire.

Figure 5.- Concluded.
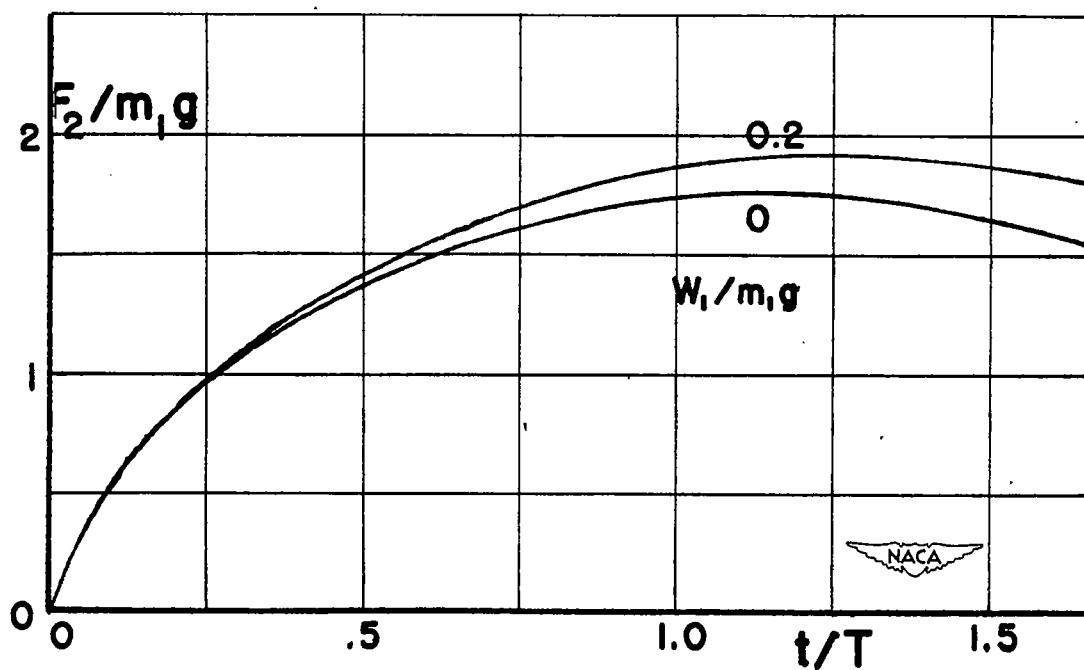
Figure 6.- Influence of weight and lift on landing impact.
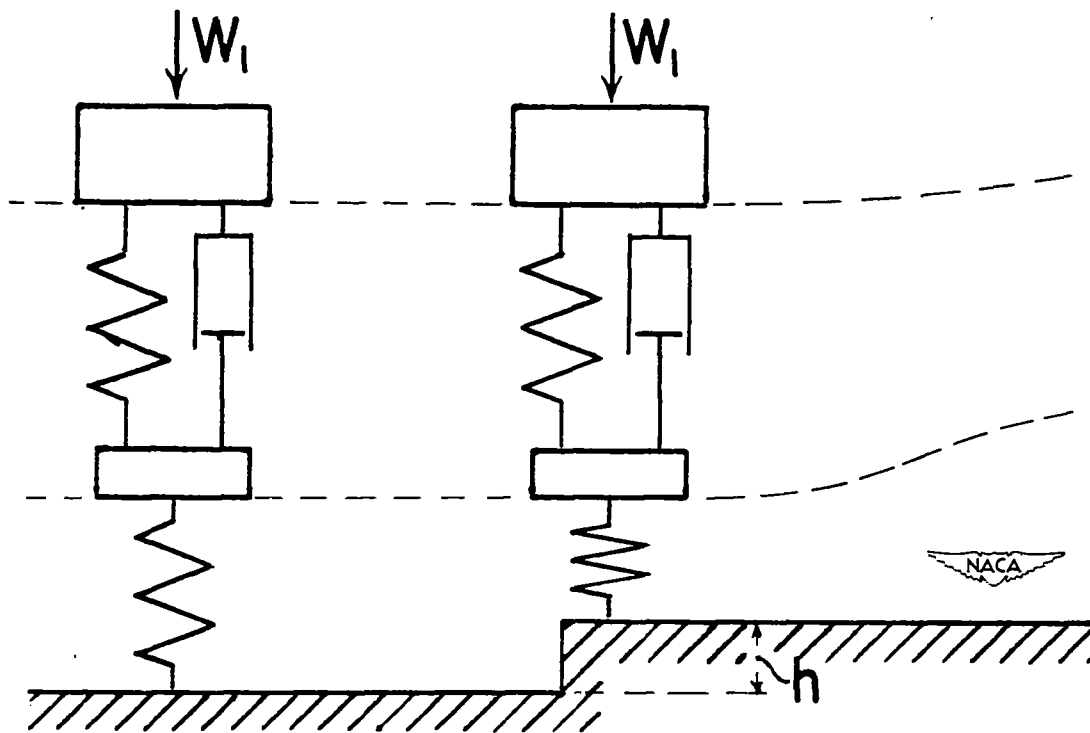
Figure 7.- Landing gear encountering obstacle during taxying.
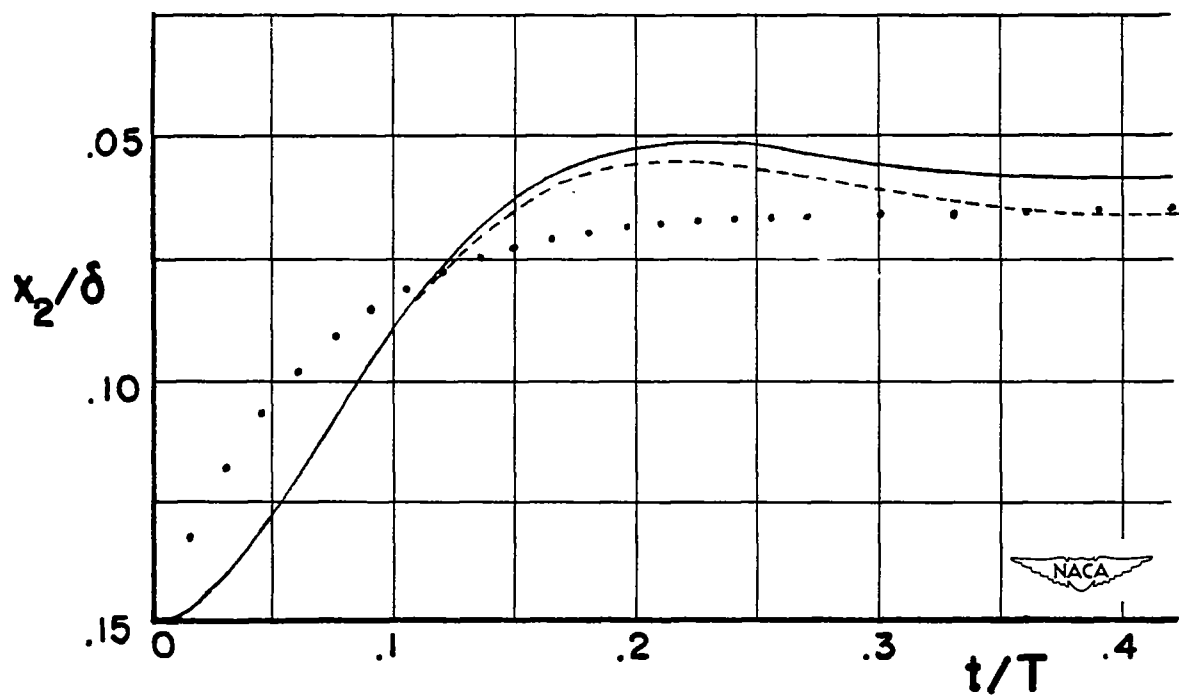
Figure 8.- Displacement of wheel when obstacle is encountered during taxying.
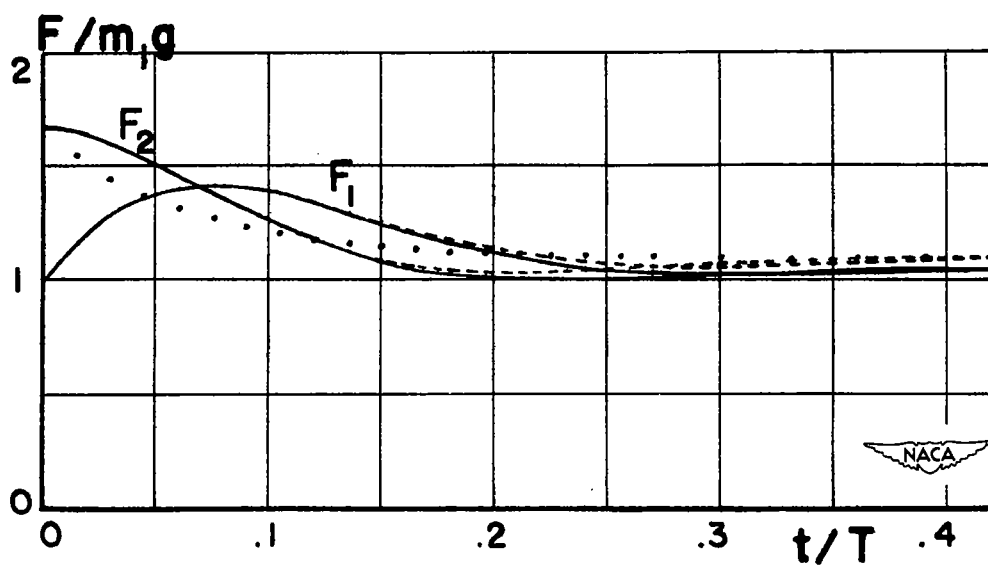
Figure 9.- Effect of encountering obstacle during taxying on forces in shock strut and in tire.

(a)   (b)
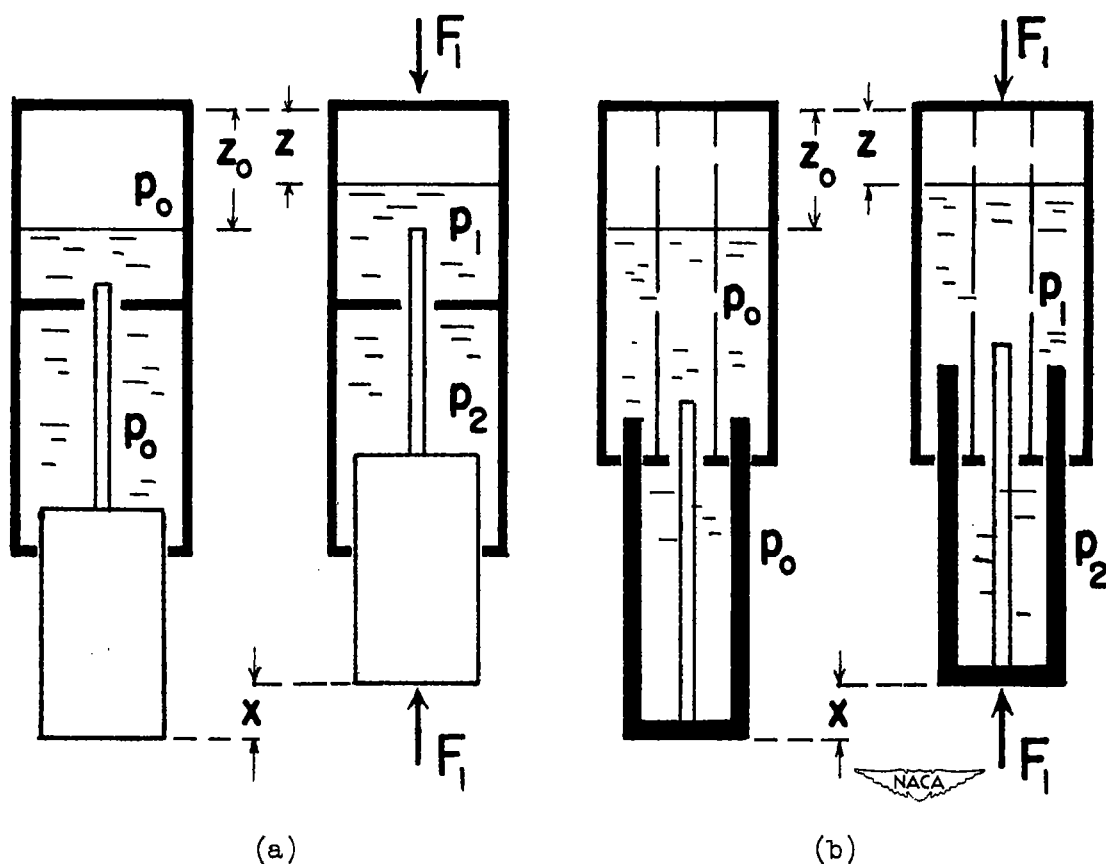
Figure 10.- Different forms of oleo struts.
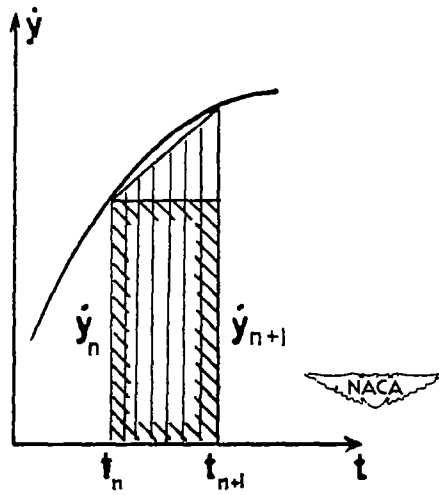
Figure 11.- Illustration of trapezoid method of integration.
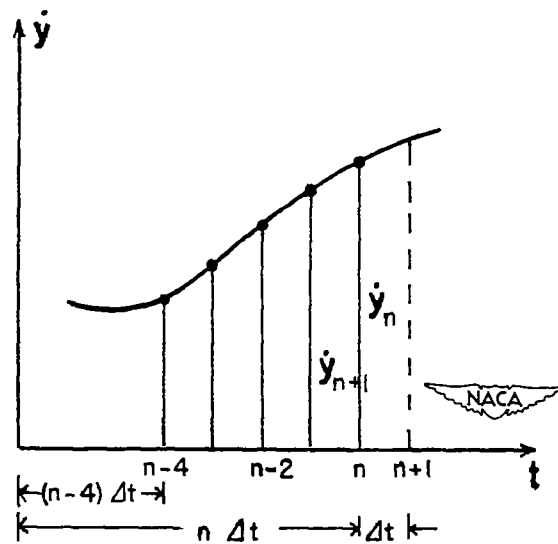
Figure 12.- Illustration of polynomial method of integration.
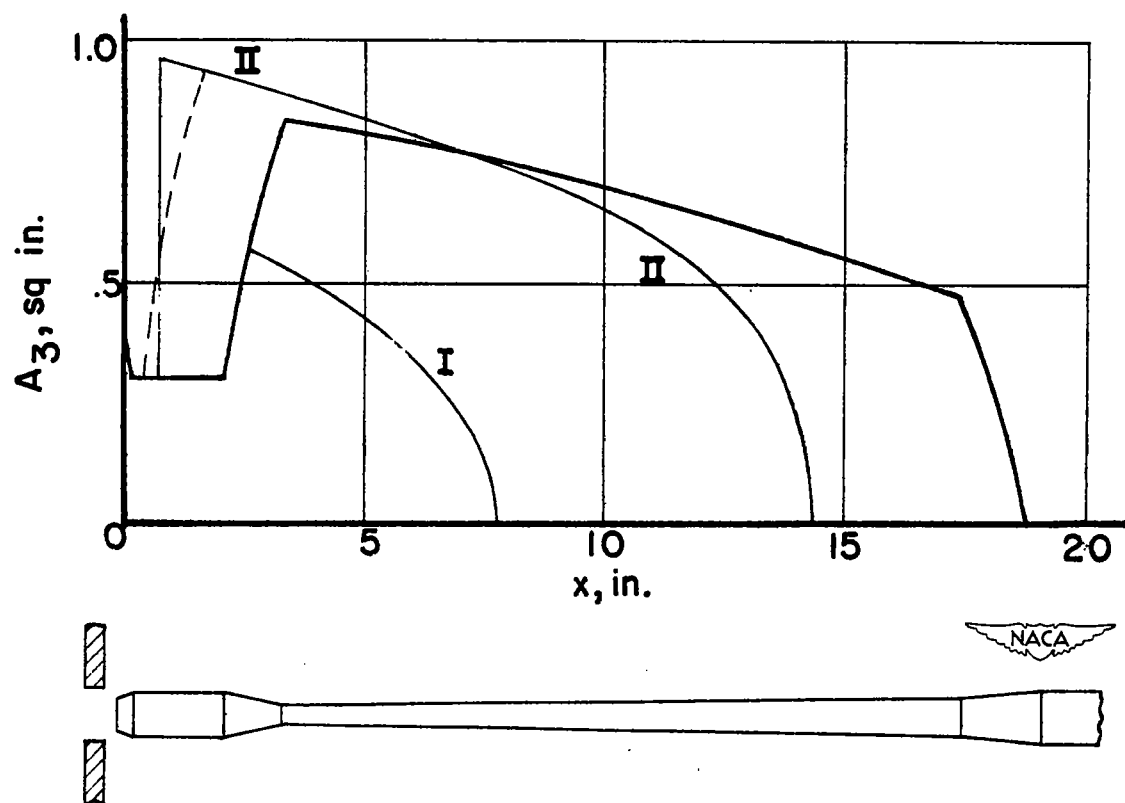
Figure 13.- Cross section of metering pin.
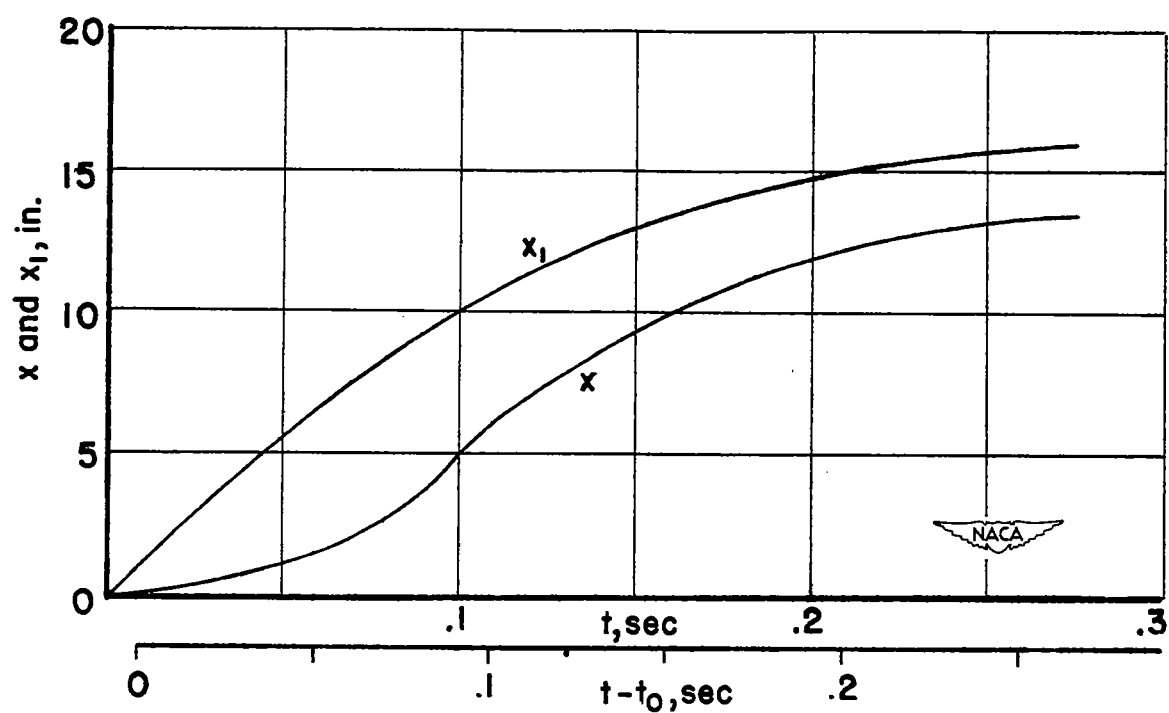
Figure 14.- Displacement x_1 and stroke x against time.
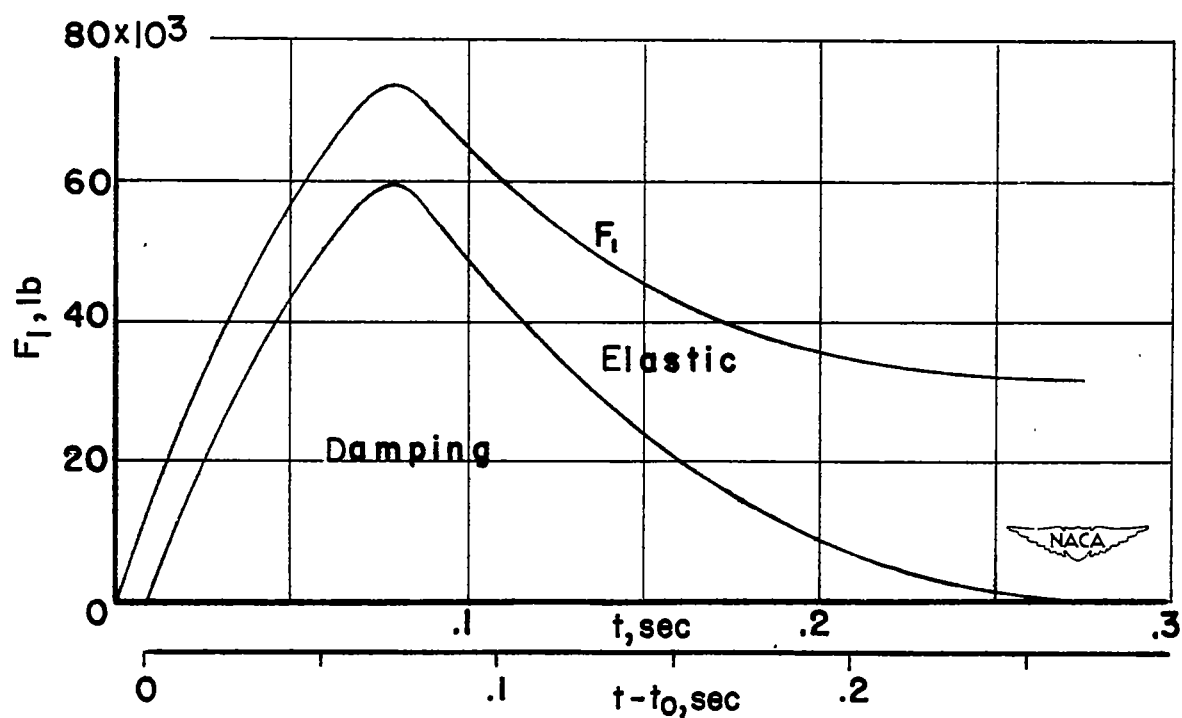
Figure 15.- Force-time history of shock strut.
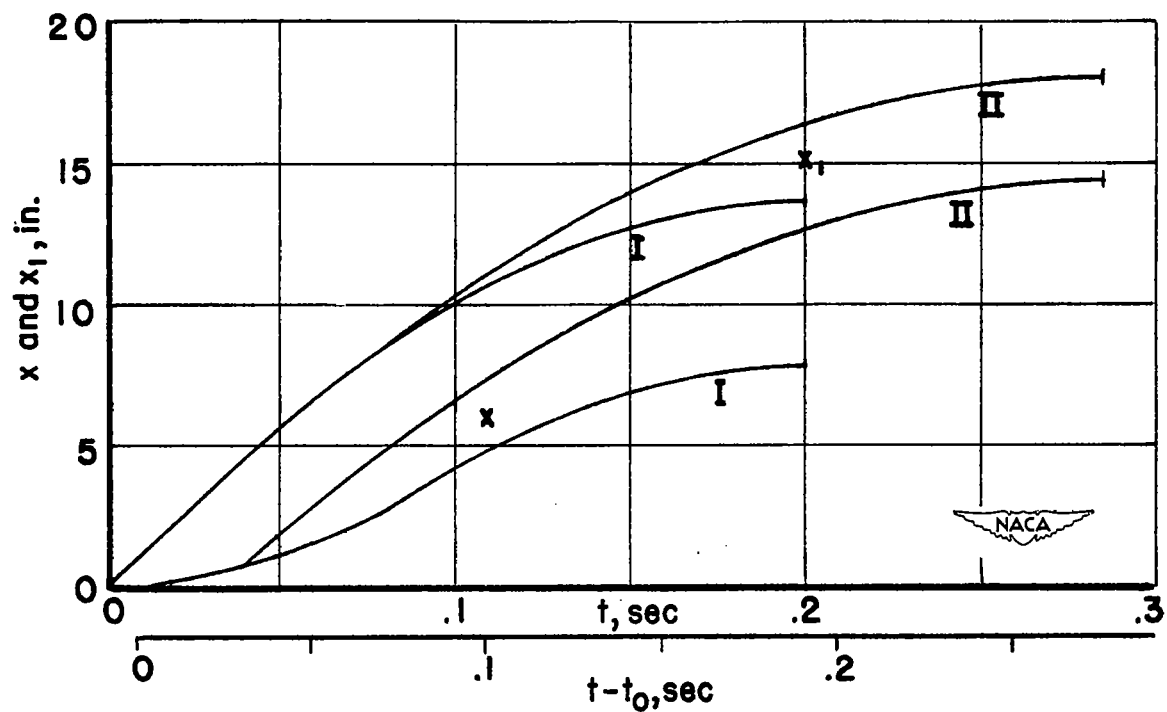
Figure 16.- Displacement x_1 and stroke x for different metering pins.
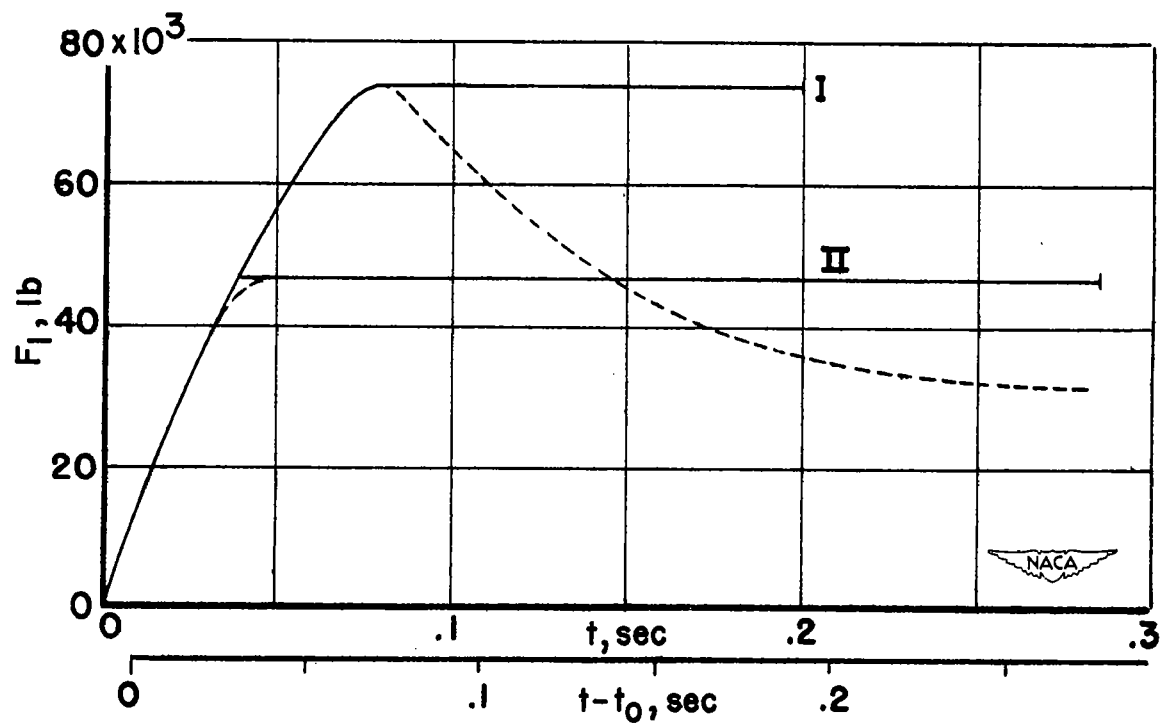
Figure 17.- Force-time history for different metering pins.
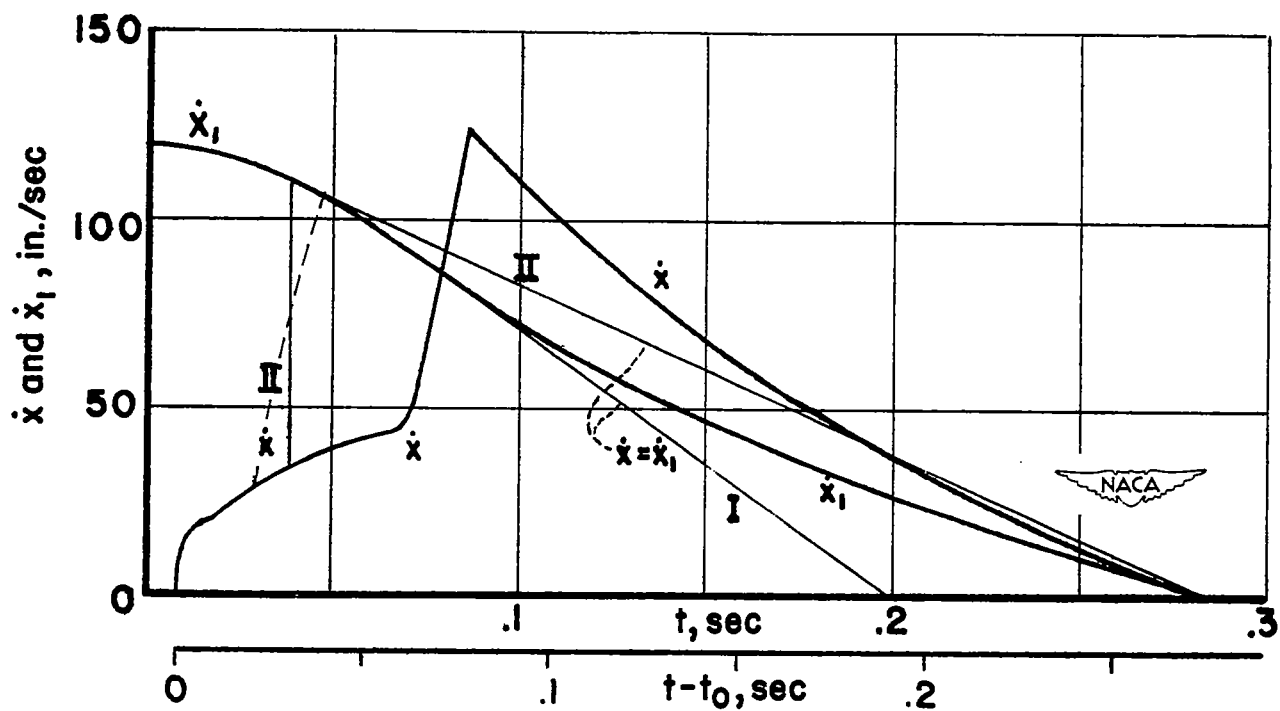
Figure 18.- Vertical velocity $\dot{x}_1$ and rate of stroke $\dot{x}$ for different metering pins.
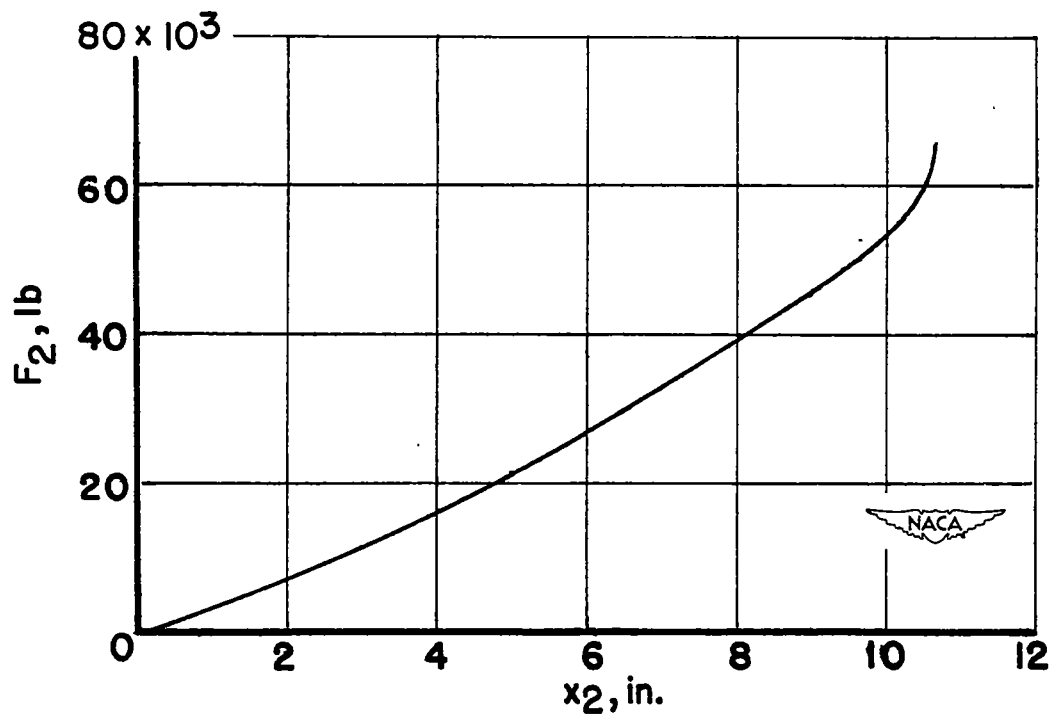
Figure 19.- Load-deflection curve of a tire.
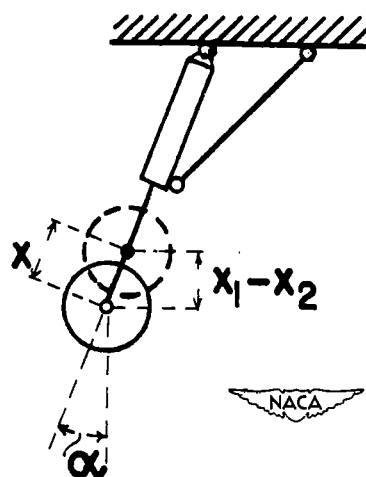
Figure 20.- Example of landing gear with shock strut inclined from vertical.
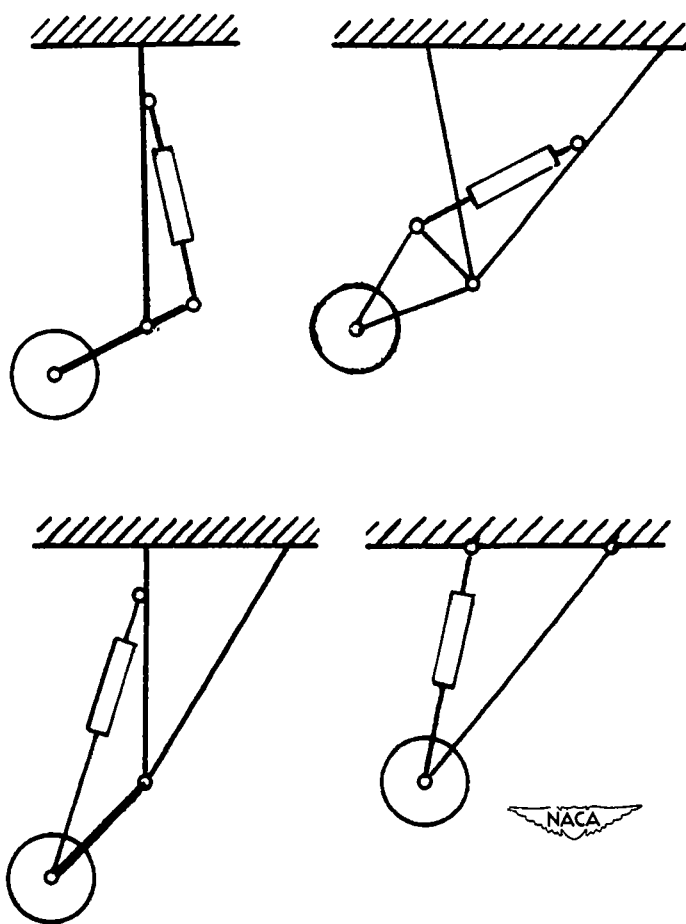
Figure 21.- Cases for which relation between stroke and displacements
is nonlinear.
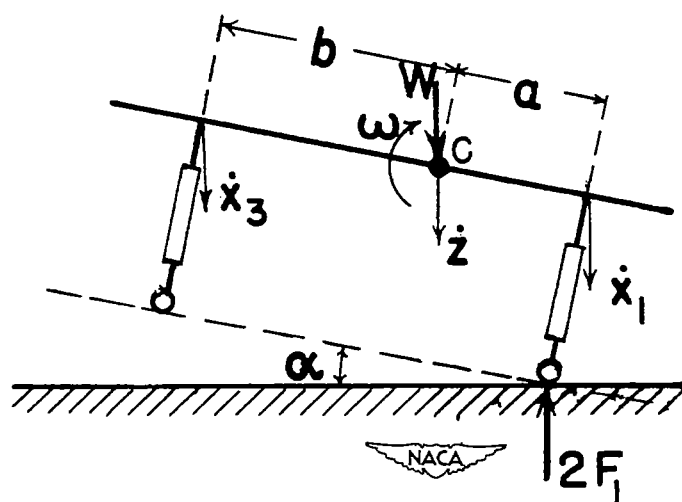
Figure 22.- Schematic side view of airplane at time of first contact.
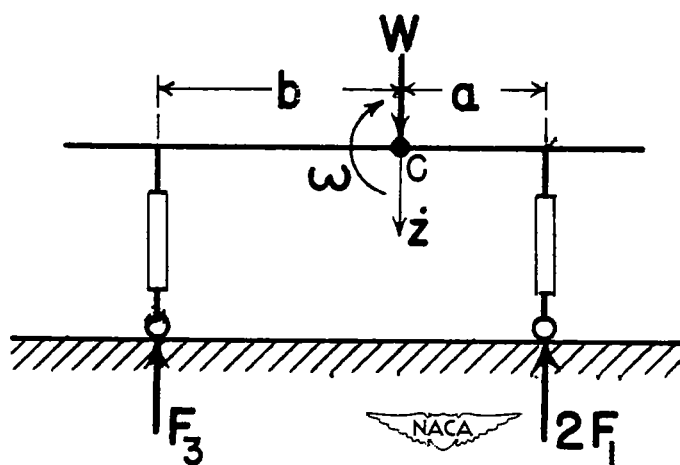
Figure 23.- Schematic side view of airplane at time
of three-wheel contact.
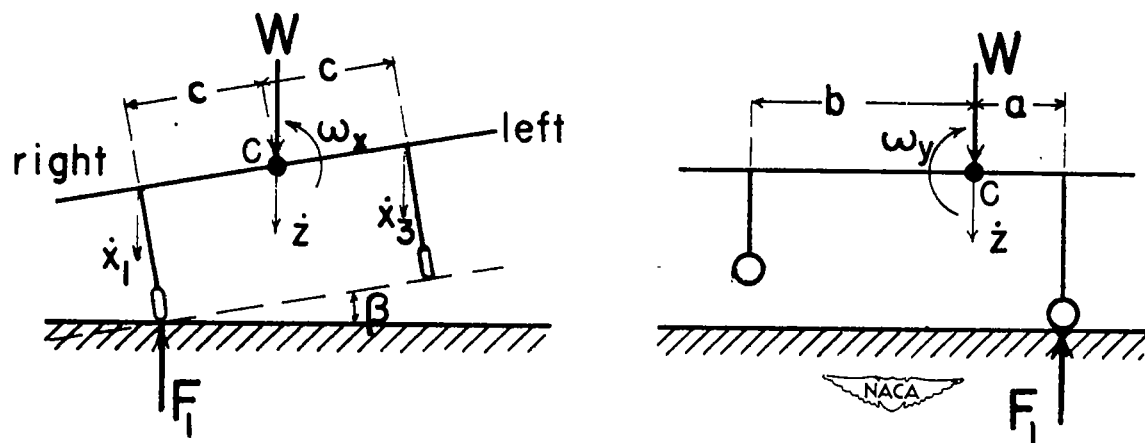
Figure 24.- Schematic views of airplane during one-wheel landing.
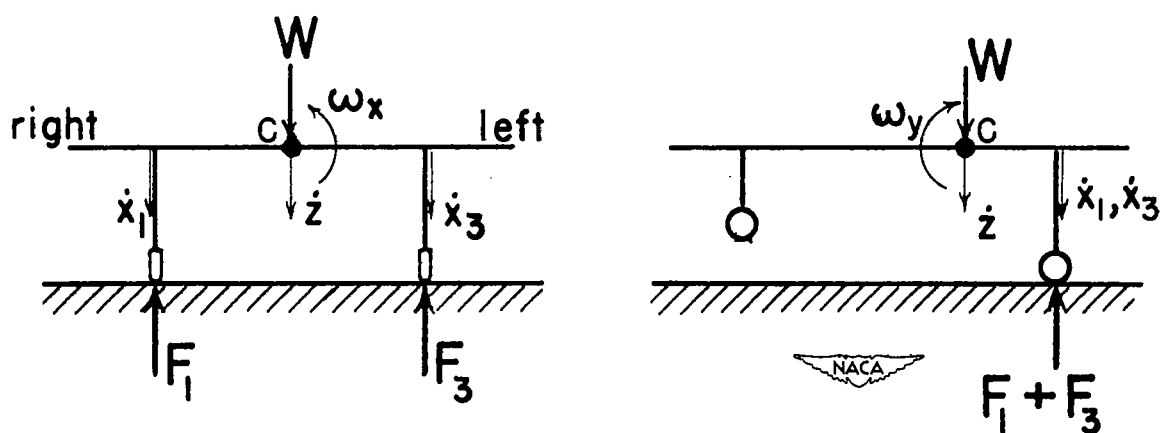Situation at first contact.

Figure 25.- Schematic views of airplane during one-wheel landing.
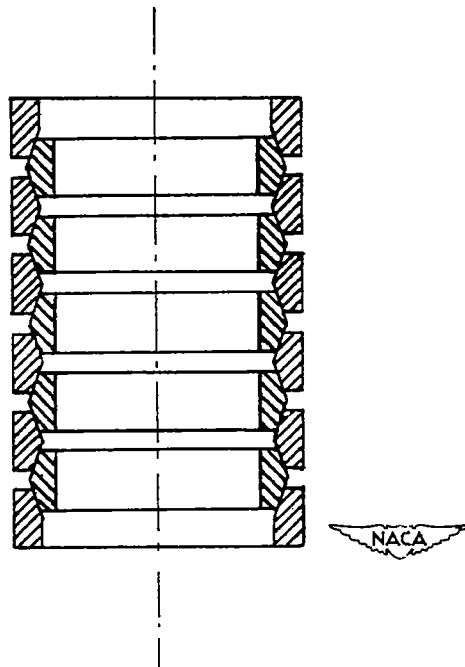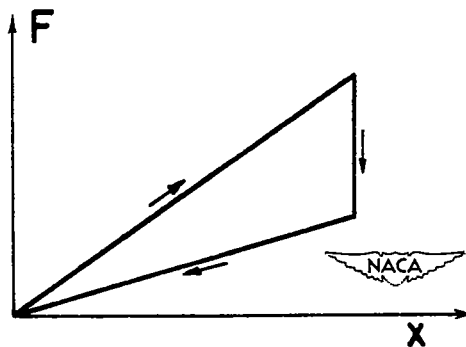Situation when second wheel hits runway.

Figure 26.- Ring-pile spring.

Figure 27.- Force-stroke diagram of a ring-pile spring.